Kent Academic Repository
Full text document (pdf)

Citation for published version

Rahman, M. Atiqur and Manser, Catherine and Benlaouer, Ouafa and Suckling, Jason and Blackburn, Jennifer K. and Silva, John and Ushkaryov, Yuri A. (2019) C-terminal phosphorylation of latrophilin-1/AD affects the interaction between its fragments.   The Annals of the New York Academy of Sciences .   ISSN 1749-6632.   (In press)

DOI

Link to record in KAR

https://kar.kent.ac.uk/76429/

Document Version

Author's Accepted Manuscript

C-terminal phosphorylation of latrophilin-1/ADGRL1 affects the interaction between its fragments

M. Atiqur Rahman[1], Catherine Manser[1], Ouafa Benlaouer[2], Jason Suckling[1,3], Jennifer K. Blackburn[2,4], John Silva[1,5], and Yuri A. Ushkaryov[1,2,6]

[1]Department of Life Sciences, Imperial College London, London, SW7 2AZ, UK

[2]School of Pharmacy, University of Kent, Chatham, ME4 4TB, UK

[3]Current address: Thomsons Online Benefits, Gordon House, 10 Greencoat Place, SW1P 1PH, London, UK

[4]Current address: Division of Molecular Psychiatry, Yale University School of Medicine, New Haven, CT 06510, USA

[5]Current address: Department of Bioanalytical Sciences, Non-clinical development, UCB-Pharma, Slough, Berkshire, SL1 3WE, UK

[6]To whom correspondence should be addressed

Address for correspondence: y.ushkaryov@kent.ac.uk. School of Pharmacy, University of Kent, Chatham, ME4 4TB, UK

Short title: Phosphorylation of latrophilin-1

Key words: latrophilin, adhesion GPCRs, fragment, phosphorylation, α-latrotoxin

Abstract

Latrophilin-1 is an Adhesion G protein-coupled receptor, which mediates the effect of α-latrotoxin, causing massive release of neurotransmitters from nerve terminals and endocrine cells. Autoproteolysis cleaves latrophilin-1 into two parts: the extracellular N-terminal fragment (NTF) and the heptahelical C-terminal fragment (CTF). NTF and CTF can exist as independent proteins in the plasma membrane, but α-latrotoxin binding to NTF induces their association and G protein-mediated signaling. We demonstrate here that CTF in synapses is phosphorylated on multiple sites. Phosphorylated CTF has a high affinity for NTF and co-purifies with it on affinity columns and on sucrose density gradients. Dephosphorylated CTF has a lower affinity for NTF and can behave as a separate protein. α-Latrotoxin (and possibly other ligands of latrophilin-1) binds both to the NTF-CTF complex and to receptor-like protein tyrosine phosphatase σ, bringing them together. This leads to CTF dephosphorylation and facilitates CTF release from the complex. We propose that ligand-dependent phosphorylation-dephosphorylation of latrophilin-1 could affect the interaction between its fragments and its functions as a G protein-coupled receptor.

Introduction

Latrophilin (LPHN1, or ADGRL1 in the new nomenclature[1]) is a classical representative of Adhesion G protein-coupled receptors (Adhesion GPCRs). It was discovered due to its interaction with α-latrotoxin (α-LTX) from black widows spider venom[2–5]. Latrophilin was one of the first GPCRs to be recognized as an unusual receptor belonging to a new group, which is now known as Adhesion GPCRs.

Adhesion GPCRs are a large family within the superfamily of GPCRs. They are ancient proteins, found in all vertebrates as well as in primitive and unicellular metazoans, and even in fungi (reviewed in Ref. 1). Adhesion GPCRs are thought to convert physical extracellular interactions into intracellular signaling and may have evolved to help cells communicate with the environment and with each other, a feature that could contribute to the evolution of multicellularity in metazoans. Adhesion GPCRs feature some unusual structural characteristics that clearly distinguish them from the rest of GPCRs: a long N-terminal extracellular domain which contains a variable number of very diverse cell-adhesion modules, a conserved extracellular "GPCR autoproteolysis-inducing" (GAIN) domain, which is unique to Adhesion GPCRs, and a long cytoplasmic C-terminal tail[6]. Autoproteolysis within the GAIN domain occurs in most members of this family and breaks the proteins into two parts: N-terminal fragment (NTF) and C-terminal fragment (CTF). The functional association and dissociation of the NTF and CTF have been first studied in LPHN1[4,7,8].

The NTF does not have a transmembrane domain, but can anchor on the cell surface by forming a strong complex with the CTF[4] or via an unknown membrane anchor[7]. In contrast, the CTF is essentially a classical GPCR[9], with a very short N-terminal ectodomain (18 amino acids)

and a long cytosolic tail (~350 residues). The very N-terminal 7 amino acids of CTF (called a *Stachel* peptide) are important for the interaction between the NTF and CTF[7,10,11].

In LPHN1, the two fragments have been shown to behave as partially independent proteins on the cell surface[7,8] (see also Discussion). All known ligands of LPHN1 (its natural agonist α-LTX and its physiological partners: teneurin-2[12], FLRT-3[13], and contactin-6[14]) interact with its NTF. At least α-LTX and teneurin-2 induce NTF and CTF association and formation of large receptor complexes, generating intracellular signals[7,8,12,15,16]. α-LTX, a potent presynaptic neurotoxin that triggers strong release of neurotransmitters from neuronal and endocrine cells[17], is the best known agonist for LPHN1 and is most useful to study LPHN1. First, it has the highest affinity for LPHN1 and does not dissociate from it during affinity chromatography under stringent conditions. Second, it is evolutionarily adapted to cause strong signaling, which cannot be achieved with more physiological ligands. Finally, most interesting facts about the LPHN1 architecture and functions have been discovered due to the use of α-LTX[17]. However, wild-type α-LTX also forms Ca^{2+}-permeable pores in biological membranes[18], creating a technical problem when detecting intracellular signaling. Therefore, a mutant LTX[N4C(19)], which does not form membrane pores[7,20], has been primarily used to study the LPHN1-mediated intracellular signaling. It has been shown[7,20–25] that LTX[N4C] binding to the NTF induces its association with the CTF and stimulates a G-protein signaling cascade (Gαq → phospholipase C (PLC) → inositol(1,4,5)trisphosphate → release of stored Ca^{2+}) and thus leads to potentiation of exocytosis.

However, very little is still known about the regulation of the CTF signaling functions. In particular, GPCRs are known to be regulated by phosphorylation[26–28], yet, to date,

phosphorylation of any Adhesion GPCRs was reported in one publication only[29], where the application of a mechanical force to the NTF of CD97 (ADGRE5) was shown to cause phosphorylation of the CTF, which altered its intracellular coupling. This suggests that CTF phosphorylation may play an important role in Adhesion GPCR functions and needs to be carefully studied.

Here, we demonstrate that the CTF of LPHN1 in neuronal nerve terminals is normally phosphorylated on multiple sites. We also show that the phosphorylated CTF species have a high affinity for the NTF and form stable complexes with it, while dephosphorylated CTF has a lower affinity for NTF and can exist separately from the NTF. The binding of α-LTX to the NTF induces NTF-CTF coupling and also recruits receptor-like protein tyrosine phosphatase σ (RPTPσ1) to the complex, leading to CTF dephosphorylation and a decrease in its affinity for the NTF. Our findings suggest that LPHN1 functioning as a two-subunit complex may be regulated by the phosphorylation of its CTF. This study provides a first glimpse into the role of phosphorylation in the dynamic structure of Adhesion GPCRs and calls for an in-depth investigation of this phenomenon.

Experimental Procedures

Materials

The following primary antibodies were used to stain LPHN1 fragments and other proteins. **NTF**: rabbit polyclonal anti-peptide antibody PAL1[30] (immune IgG against CYAFNTNANREEPVSLAFPNP); affinity-purified rabbit polyclonal antibody RL1 (against the whole rat NTF)[2]. **CTF**: affinity purified rabbit polyclonal antibody R4 (against the cytosolic tail of

rat CTF)[31]; chicken polyclonal anti-peptide IgY CCT (against C-terminal peptide CEGPGPDGDGQMQLVTSL. **Neurexin Iα**: affinity-purified rabbit polyclonal anti-peptide antibody 116-1 (produced in-house against rat peptide CSANKNKKNKDKEYYV)[31]. Receptor-like protein tyrosine phosphatase σ (**RPTPσ1**): goat polyclonal IgG against the extracellular fragment of mouse RPTPσ (R&D Systems). Antibodies recognizing **phosphorylated amino acids**: anti-phosphoserine mouse monoclonal antibody (16B4, Sigma-Aldrich); anti-phosphotyrosine mouse monoclonal antibody (2C8, Sigma-Aldrich); anti-phosphothreonine rabbit monoclonal antibody (Sigma-Aldrich). All chemical reagents were from Sigma-Aldrich, unless otherwise stated.

Fractionation of brain membranes

Male Sprague-Dawley rats (150 g) were purchased from Charles River UK. In some experiments, male C57BL/6 mice (Charles River UK) were used in parallel with the LPHN1 knockout mouse strain AG148, obtained in-house[16] and back-crossed onto C57BL/6 background. The brains were removed from animals within 30 s of Schedule 1 and homogenized with 10 strokes of a Potter-Elvehjem homogenizer (clearance 0.2 mm) in 0.32 M sucrose, 10 mM HEPES, pH 7.4, supplemented with protease inhibitors (see below). This Total Brain homogenate (TB) was centrifuged for 2 min, at 2,200 x *g* in a table-top centrifuge (Heraeus) to yield a pellet P1 (containing nuclei, large fragments of neuronal and glial cell bodies, and connective tissue) and a supernatant S1 (containing crude post-nuclear membranes: synapses, broken dendrites and axons, and somal cytosol and intracellular membranes). The S1 was further centrifuged for 20 min, at 12,000 x *g* using a Sorvall SS34 rotor (Beckman) to yield pellet P2 (containing crude post-nuclear membranes and lacking somal

cytosol and intracellular membranes), and supernatant S2 (containing cytosol, somal vesicles, and broken membranes). P2 was further separated by 1 h centrifugation at 64,000 x g on step-wise Ficoll gradients (7.5% and 12.5% Ficoll) to isolate synaptosomes[32]. The synaptosomes were recovered from the 7.5%/12% Ficoll interface. To remove the Ficoll, the synaptosomes were washed twice by resuspension/centrifugation in a physiological buffer containing (in mM): NaCl, 132; KCl, 5; $MgSO_4$, 2.5; EGTA, 0.1; D-glucose, 10; HEPES, 20 (pH 7.4). To obtain synaptosomal plasma membranes (SPM), synaptosomes were osmotically lysed in 30 ml of ice-cold 10 mM Tris-HCl, pH 7.6, containing 50 µM $CaCl_2$ and protease inhibitors. The lysate was subjected to three freeze/thaw cycles at -70 ºC, after which it was centrifuged for 1 h, at 100,000 x g, at 4 ºC, to yield SPM and supernatant S3. S3 was used for synaptic vesicle purification. All membrane fractions were used for LPHN1 purification (see below).

Affinity purification of LPHN1

An α-LTX column was synthesized by immobilizing 1 mg of highly purified α-LTX[33] on 1 mL of CNBr-activated Sepharose-4CL (Sigma-Aldrich). To optimize LPHN1 extraction, different detergents (Thesit, Triton X-100, or CHAPS) were tested. Respective membrane pellets were re-suspended in TBS buffer (50 mM Tris-HCl, pH 7.6, 0.2 M NaCl) containing 2 mM EDTA and 2% detergent, incubated for 2 h, at 4ºC, then centrifuged for 20 min, at 20,000 x g and the supernatants were mixed with a 6X loading buffer for SDS-polyacrylamide gel-electrophoresis (SDS-PAGE) (see below). Thesit proved to be optimal for LPHN1 extraction and was used in all affinity chromatographies. All buffers also contained protease inhibitors: 104 mM AEBSF, 80 µM aprotinin, 4 mM bestatin, 1.4 mM E-64, 2 mM leupeptin and 1.5 mM pepstatin A (Sigma-Aldrich). As described under Results, a phosphatase inhibitors (PPI) cocktail (final

concentrations: 2 mM imidazole, 1 mM NaF, 1.2 mM sodium molybdate, 1 mM sodium orthovanadate, and 4 mM sodium tartrate dihydrate) (Sigma-Aldrich), or at least 100 mM activated sodium orthovanadate, was added where appropriate. The solubilized membranes were cleared by centrifugation for 20 min, at 20,000 x g and diluted 3-fold with TBS. Preparative affinity chromatography of LPHN1 was carried out on a freshly prepared 1-mL α-LTX-column; analytical purification of LPHN1 from the lysates obtained from different membrane fractions was conducted using 50 µL of the α-LTX-column. The lysates were incubated with the α-LTX column overnight, at 4ºC. The beads were then washed with 50 column volumes of TBS containing 0.2% Thesit (TBT), then with 20 column volumes of 0.5 NaCl in TBT and then eluted with 2 M NaCl in TBT or with SDS-PAGE Sample Buffer to ensure complete removal of LPHN1 from the gel matrix.

For additional LPHN1 purification, diluted high salt eluates from α-LTX affinity chromatography (or synaptosomes solubilized as described above) were incubated with 1 ml of wheat germ agglutinin (WGA)-Sepharose 4B (Sigma-Aldrich) for 16 h, at 4ºC. The gel was then extensively washed with 0.5 M NaCl in TBT, followed by elution with 100 mM N-acetylglucosamine or SDS-containing sample buffer, as specified under Results.

LPHN1 deglycosylation

LPHN1 isolated by LTX affinity chromatography was resuspended in TBT containing 2 mM CaCl$_2$ and treated with 10 mU of neuraminidase (Boehringer Mannheim) for 1 h, then denatured for 10 min with 1% SDS, supplemented with 1% Triton X-100 to neutralize SDS, and finally treated for 1 h with peptide:N-glycosidase F (PNGase, Boehringer Mannheim) and/or O-

glycosidase (Calbiochem). All incubations were performed at 37ºC and stopped by adding SDS-PAGE Loading Buffer.

Immunoprecipitation

Purified LPHN1 was incubated with a chicken antibody against a rat CTF peptide (see above), overnight, at 4ºC, with rotation. Protein A-Sepharose 4B (Sigma-Aldrich) was added to this mixture and incubated for 2 h, at 4ºC. The beads were washed with 0.5 M NaCl in TBT and eluted with a 2x SDS sample buffer, before being heated for 30 min at 50ºC and loaded on an SDS-gel.

Sucrose density gradients

Sucrose density gradient centrifugation was performed essentially as described previously[34]. The gradients consisted of 10 layers of 8 to 17% (w/v) sucrose in TBT and an underlying 1 ml cushion of 30% sucrose. These step-wise gradients achieved perfect linearity after centrifugation, which was controlled by measuring the density of all fractions. 1-ml samples of solubilized membranes were loaded on the top of gradients, which were centrifuged for 16 h at 165,000 x g in an SW40Ti rotor, at 4ºC. After centrifugation, 0.5-ml fractions were collected, starting from the bottom of the tube, and analyzed by SDS-PAGE and Western blotting.

CTF dephosphorylation

Purified native LPHN1 was treated at 37ºC for 1 h with 1 unit of a recombinant alkaline phosphatase (Sigma-Aldrich) in the presence of 5 mM Tris, pH 9.8, 1 mM $MgCl_2$ and 0.1 mM

ZnCl$_2$. Samples were collected at regular time intervals, titrated to pH 6.8, and analyzed by SDS-PAGE and Western blotting. PPI cocktail (see above) was used in some experiments.

LPHN1 ^{125}I-iodination

LPHN1 was purified from P2 membranes on an α-LTX-column in the presence of protease inhibitors and PPIs, as described above, and eluted from the column with TBT containing 2 mM EDTA and 2 M NaCl. The receptor was then desalted on a Bio-Gel P-10 column (Bio-Rad) equilibrated in TBT and concentrated to ~54 nM using centrifugal ultrafiltration units (Amicon Ultra-15, Merck), at 4°C. A 100-μL aliquot of this solution containing 1 μg of LPHN1 was mixed with 5 μL Na^{125}I (18.5 MBq), 7.5 μL of 2.8 mM chloramine T and TBT to 150 μL, and incubated for 1 min, with periodic up-down pipetting. The reaction was stopped by the addition of 7.5 μL of 3.7 mM Na$_2$S$_2$0$_5$ and 50 μL of 160 mM NaI in TBT, mixed and immediately loaded on the top of a Bio-Gel P-10 column pre-equilibrated in TBT containing 0.1% BSA. The column was eluted by sequential addition of 0.5 mL aliquots of TBT to the gel top and collection of respective fractions. Fractions (2-6) containing the radioactive protein were combined; protein recovery was about 90% in non-radioactive pilot experiments.

LPHN1 ^{32}P-phosphorylation

Synaptosomes (Syn) were isolated from rat brain cortex, as described above, resuspended in 5 mL of buffer containing (in mM): NaCl, 140; KCl, 3; MgCl$_2$; 1, CaCl$_2$, 2; D-glucose, 5.6; HEPES-NaOH, 10, pH 7.4; and equilibrated at 23°C for 10 min, with constant oxygenation. The reaction was initiated by adding [^{32}P]orthophosphate (18,5 MBq). The final concentrations of PO$_4$$^{3-}$ was 1 μM. The reaction proceeded for 1 h and was terminated by the addition of an equal

volume of ice-cold PBS containing 2% Triton X-100, 20 mM EDTA and PPIs. After a 2 h incubation at 4°C, solubilized proteins were cleared by centrifugation at 20,000 x g for 20 min, at 4°C. The lysate was diluted to 0.2% Thesit and incubated with a 50 μL LTX-column for 2 h, at 4°C; the column was washed and eluted with SDS Loading Buffer. The proteins were then resolved by SDS-PAGE and visualized by autoradiography and Western blotting. Prior to SDS-PAGE, some samples were boiled for 5 min (see Results).

[^{32}P]-Phosphorylation of COS7 cells, transiently transfected with LPHN1 or an empty vector, was carried out by adding $^{32}PO_4^{3-}$ (18.5 MBq) to the culture medium 6 h after transfection, followed by overnight incubation at 37°C and 5% CO_2. The cells were harvested from the plates in PBS containing 1% Thesit, incubated for 1 h, centrifuged at 20,000 x g, at 4°C, and the supernatants were analyzed by SDS-PAGE and Western blotting.

SDS-gel electrophoresis

Discontinuous SDS-PAGE was performed according to Laemmli[35] using BioRad Mini-Protean II apparatus. Liquid protein samples were mixed with 2X-6X Loading Buffer, which contained 100 mM dithiothreitol (DTT) (final concentration). Before loading onto gels, samples were heated for 2-5 min at 100ºC or for 30 min at 37-50ºC. To perform SDS-PAGE in the presence of urea, the resolving gel, stacking gel and loading buffer were supplemented with electrophoresis grade 8 M urea (Sigma-Aldrich). Protein samples containing urea were only heated to 37ºC. Electrophoresis was carried out at 100 V and, when the samples reached the resolving gel, at 150 V.

Prior to SDS-PAGE dilute samples were concentrated by protein precipitation, according to one of the following methods. Method 1: two volumes of a 1:1 chloroform/methanol mixture was added to one volume of sample, followed by thorough mixing and a brief centrifugation. The precipitate recovered from the solvent-water interface was washed once with methanol and then dried in air. Method 2: ice-cold trichloroacetic acid was added to samples to a final concentration of 10%, the mixture was left on ice for 20 min and then centrifuged for 30 min, at 25,000 x g and 4°C. After the removal of the supernatant, the pellet was washed with ice-cold acetone, then dried in air. Resulting sample pellets were dissolved in 1X Loading Buffer and heated as described above.

Western blotting

Proteins separated in SDS-gels were transferred onto polyvinylidene fluoride (PVDF) membranes, using a wet electrophoretic transfer unit, in a Tris-glycine buffer containing 20% methanol. The membranes were blocked using 5% non-fat milk (or 3% BSA), 0.1% Tween in PBS (PBST) overnight and washed 5 times with PBST. The blots were then incubated for 1 h with respective primary antibodies, washed 5 times with PBST and incubated for 1 h with matching horseradish peroxidase-conjugated secondary antibodies (Sigma-Aldrich). After additional 5 washes with PBST, the immunostained proteins were visualized using the enhanced chemiluminescence technique, as specified by the manufacturer (Millipore).

The images were obtained by exposure to Kodak BioMax XAR film (Sigma-Aldrich) or digitally captured using a LAS-3000 gel imager at a maximal resolution (Fujifilm). Multiple exposures were taken to determine the linear response range of the film/detection camera for each protein. Radioactive proteins were detected by exposure of the blots to Kodak BioMax XAR film over

16-72 h; ^{32}P exposure was carried out at -70°C using an intensifying screen. Exposed film was digitized by optical scanning at 600-1200 dpi resolution, in the transparency mode. Digitized images were analyzed by computer-aided densitometry using the image processing software Fiji (NHS).

Affinity purification of anti-NTF and anti-CTF antibodies

For affinity purification of RL1 and R4 antibodies, expression constructs were made containing, respectively, rat NTF (nucleotides 630–2957) fused with glutathione-S-reductase and rat CTF cytosolic tail (nucleotides 3976–4856) fused with dihydrofolate reductase. These constructs were expressed in *E. coli*, isolated by affinity chromatography on, respectively, a glutathione column and a Ni^{2+} column, separated by SDS-PAGE and transferred onto PVDF membranes. The membranes were blocked with 5% non-fat milk in PBST and incubated with the respective antisera overnight. After several washes with PBS, specific antibodies were eluted from the membranes with 0.5 M NaCl, 0.5 M glycine, pH 2.4, and neutralized with Tris base.

Cell culture

African green monkey kidney (COS7) and mouse neuroblastoma (NB2a) cell lines were maintained at 5% CO_2, 37°C, in multi-well plates (Nunc) in Dulbecco's modified Eagle's medium (Life Technologies, Inc.) containing 10% fetal bovine serum (NB2a cells were also supplemented with Glutamax^{TM}). Cells were grown to 80% confluence and split 1:6 every 2-3 days. When passaging, the cells were detached using Trypsin-EDTA (0.05 %). Cells were transiently transfected with full-size LPHN1 in pcDNA3.1[7] using the SuperFect transfection reagent (Qiagen), according to the manufacturer's protocol, and analyzed 24 h later. Stable

lines were generated in NB2a cells by FuGene6-aided transfection (Roche Diagnostics), followed by G418 (Invitrogen) selection and cell sorting (Becton Dickinson). Stably transfected NB2a cell lines were maintained in G418 (300 μg/mL).

Protein phosphorylation bioinformatics

The following Internet resources were used to predict phosphorylation consensus sites in the full CTF sequence: PhosphoSitePlus (https://www.phosphosite.org/homeAction.action)[36], NetPhos 2.0 (http://www.cbs.dtu.dk/services/NetPhos-2.0/); NetPhos 3.1b (http://www.cbs.dtu.dk/services/NetPhos/); PhosphoMotif Finder (http://www.hprd.org/PhosphoMotif_finder); KinasePhos (http://kinasephos.mbc.nctu.edu.tw/predict.php) and some other. Potential phosphorylation sites detected by the software in the extracellular loops were disregarded.

Reverse-transcription polymerase chain reaction (RT-PCR)

Total RNA from NB2a cells was isolated using a High Pure RNA Isolation Kit (Roche). RNA concentration and purity was assessed with a Nanodrop 2000 spectrophotometer (Thermo Fisher Scientific). cDNA was synthesized using 1 μg total RNA and anchored oligo(dT)18 primers with the Transcriptor First Strand cDNA Synthesis Kit (Roche). Expression profiles of RPTPS1, STIM1, STIM2, and β-actin mRNA were determined using quantitative RT-PCR (qRT-PCR) performed on a LightCycler 480 (Roche) using SYBR GreenIMaster reaction mix (Roche) and specific primers designed using the Lasergene software (DNASTAR) (target gene RPTP1S, CCGCTATGTCCTCTTTGTGCTTGC / GCGGGGCTCTGAGTCCTTGCGTTT; housekeeping gene β-actin, TTCGCGGGCGACGATGC / GGGGCCACACGCAGCTCATT; control genes STIM1, CCGCCCTAACCCCGCCCACT / CCCCCTCAATCAGCCGATGGC and

STIM2 TCAGCCGGCAATGATAGCAAG / TGGAAAGCCCCAGTGGAGTTA). Reactions began with a 5 min preincubation at 95°C, followed by 40-45 cycles of 10 s at 95°C, 20 s at 60°C, and 10 s at 72°C. A final elongation step at 72°C continued for 5 min. Fluorescence was measured once at 80°C during each cycle. Amplification of correct products was confirmed using the LightCycler melting temperature (Tm) analysis. Raw fluorescence data were analyzed using LinRegPCR quantitative PCR data analysis program[37], which calculated the PCR efficiency for each reaction. The initial amount of target cDNA in a sample was determined using the following equation: $N_0 = N_t/E_{mean}^{Cq}$, where N_0 is the initial concentration in arbitrary fluorescent units; N_t is a fluorescence threshold; E_{mean} is the mean reaction efficiency; and C_q is the quantification cycle threshold (when the reaction exceeds the initial concentration, N_0). For each reaction, the baseline fluorescence was subtracted from the curve. The specificity of qRT-PCR was ascertained by including two controls with each reaction: 1 µL of undiluted total RNA (to test for residual genomic DNA) and 1 µL of nuclease-free water (to show the specificity of cDNA amplification).

Statistical methods

The numerical data presented in Figures or text are the means ± SD. The *p* value was calculated using a two-tailed heteroscedastic t-test, with Bonferroni correction in cases of multiple pair-wise comparisons. The number of independent experiments *n* was between 3 and 12, and is demonstrated by individual data points in the diagrams. The following notation was used to denote statistical significance: NS (non-significant), $p > 0.05$; *, $p < 0.05$; **, $p < 0.01$; ***, $p < 0.001$. All images are representative of a number of independent experiments (n = 3-21), which all gave similar results; the specific *n* for each image is provided in Figure legends.

RESULTS

The CTF is phosphorylated on multiple sites

LPHN1 can be highly purified from rat brain membranes using an α-LTX affinity column[2]. To analyze possible post-translational modifications of the CTF, it was necessary to optimize its SDS-PAGE analysis (Fig. 1). As previously described[4], in conventional SDS-PAGE, only the NTF can be fully resolved as a band with an apparent molecular mass of ~ 120 kDa, while the CTF aggregates and does not enter the gel (Fig. 1A, left). Inclusion of 8 M urea in SDS-gels and loading buffer[4] allows CTF separation (Fig. 1A, middle). However, on SDS-urea gels both the NTF and CTF show abnormal mobility, appearing as diffuse, poorly resolved bands (Fig. 1A, middle). Interestingly, SDS-PAGE samples containing urea must not be boiled to avoid carbamylation of proteins, while normal SDS-PAGE samples are routinely boiled. We hypothesized that it was sample boiling (rather than a lack of urea) that caused CTF aggregation on normal SDS-gels. Indeed, when LPHN1 sample was heated to 37-50ºC only, both of its fragments were perfectly resolved in normal SDS-gels containing no urea (Fig. 1A, right). Under these conditions, the NTF appeared as a defined band of 120 kDa, while the CTF migrated at 65-75 kDa. Furthermore, the CTF was now clearly resolved into at least 4 distinct bands (Fig. 1A, inset). The relative abundance of the major bands (CTF-a,b,c,d) varied between different samples (Fig.1B) (see below).

The nature of the CTF bands was not immediately clear. One possibility was that, in addition to LPHN1, LTX-affinity columns could also pull down LPHN2 and 3. The three homologous CTFs could have different electrophoretic mobilities and could be recognized by our anti-CTF antibodies, giving rise to multiple bands. To rule out this possibility, we performed LTX-affinity

chromatography of solubilized P2 membranes from the brains of wild-type and LPHN1 knockout mice (Fig. 1C). This experiment demonstrated that mouse CTF had a similar migration pattern on SDS-gels as the rat protein, but our anti-CTF antibody did not recognize any proteins in the brains that lacked LPHN1 (Fig. 1C, arrowhead). This clearly indicated that the multiple bands stained by the anti-CTF antibody belonged to the CTF of LPHN1 only.

The other possibility was that the CTF could be post-translationally modified, e.g. glycosylated or phosphorylated. Treatment of purified LPHN1 with a set of glycohydrolases (Fig. 2A) reduced the apparent molecular mass of NTF from 120 kDa to around 105 kDa. Glycosylation of the native NTF was confirmed by extended SDS-PAGE in a 4% gel (Fig. 2A, inset). However, there was no change in the migration profile of the CTF, indicating that it was probably not glycosylated (Fig. 2A). To test for possible phosphorylation, purified LPHN1 was treated with alkaline phosphatase, an enzyme that dephosphorylates proteins modified by all types of phosphorylation. As a result, the NTF migration was not affected (Fig. 2B), while the electrophoretic mobility of the upper three CTF bands gradually increased and all CTF eventually migrated as one thick band at the level of CTF-a or slightly lower (65 kDa, Fig. 2B, lane 4; Fig. 2C). The specificity of dephosphorylation reaction was confirmed by the inclusion of PPIs, which prevented the change in CTF migration pattern (Fig. 2B, lane 5). The phosphatase also affected the CTF bands when it was applied to solubilized brain membranes, indicating that the CTF bound to its normal partners was still accessible to phosphatases. Computer-aided densitometry (Fig. 2C) indicated that the optical density of the dephosphorylated CTF band, on average, matched the density of the combined original four CTF bands, proving that they all represented one protein with different degrees of phosphorylation. The apparent size of the dephosphorylated CTF-a corresponded to that of the

CTF from recombinant LPHN1 expressed in COS7 cells (Fig. 2D, lane 1), which traveled as a single band and had either no phosphorylation or a low degree of phosphorylation.

However, even after 2 h exposure to a large concentration of alkaline phosphatase, the CTF dephosphorylation seemed to be incomplete, with a fainter secondary band appearing above the main CTF band (Fig. 2B, lane 4; 2D, lane 4). We hypothesized that this was due to a phosphate group (or groups) resistant to alkaline phosphatase, or to a different type of modification, e.g. palmitoylation. When this partially dephosphorylated CTF was treated with 0.5 M hydroxylamine, which cleaves Cys-palmitoyl thioester linkages, the residual phospho-band disappeared (Fig. 2D, lane 5). Hydroxylamine itself did not change the migration pattern of fully phosphorylated CTF (lane 6), but made it more susceptible to alkaline phosphatase (lane 7), indicating that CTF could indeed be S-palmitoylated.

When CTF was dephosphorylated, its amount often decreased on the blots (Fig. 2D, lane 2 vs. lanes 3-5), suggesting that the removal of phosphate groups could render the CTF susceptible to proteolytic degradation. However, this was unlikely, because all our buffers contained protease inhibitors, and the remaining dephosphorylated band appeared to be stable in solution. Moreover, we noticed (Fig. 2D, right) that CTF dephosphorylation greatly increased its SDS-resistant dimerization (arrowhead 2) and formation of higher complexes. When all CTF bands (including its aggregates, but excluding any fragments) were combined and normalized to NTF, no loss of CTF bands was observed (Fig. 2E). Thus, CTF dephosphorylation does not cause its degradation, but may induce it to form very stable complexes.

The type of CTF phosphorylation was revealed by staining the protein with antibodies against phosphotyrosine, phosphothreonine, and phosphoserine (Fig. 2F, lanes 4, 6, 8). This showed

that all three types of phosphorylation were present in the CTF. Even the fastest migrating band (CTF-a) appeared to carry more than one phosphate group, on both Tyr and Ser residues (lanes 4 and 8). The slow migrating bands (CTF-b,c,d) demonstrated differential phosphorylation, but most had all three types of phosphoamino acids and, thus, were phosphorylated on multiple sites. Analysis of the phosphorylation pattern (not shown) suggested that a minimum of 7 phosphates could be present in the top band (CTF-d). Alkaline phosphatase treatment removed all phosphates from the CTF (Fig. 2F, lanes 3, 5, 7), but the fully dephosphorylated CTF migrated on the gel marginally lower than the partially phosphorylated CTF-a (Figs. 2B, D, F).

To study the dynamics of CTF phosphorylation in nerve terminals, we used radioactive phosphate to evaluate the rate with which new phosphate groups could be incorporated into the CTF. For this purpose, we incubated freshly purified synaptosomes with [^{32}P]-orthophosphate for 1 h and then isolated the receptor on an α-LTX column in the presence of PPIs, to avoid LPHN1 dephosphorylation by cellular phosphatases. Pure LPHN1 was then separated by SDS-PAGE, transferred onto PVDF membrane and exposed to autoradiography film (Fig. 2G, lane 1). The following additional experiments were conducted in parallel: (1) after autoradiography, the ^{32}P-labeled membrane was immunostained for CTF and NTF (Fig. 2G, lanes 3, 5); (2) the CTF blot was additionally exposed for a longer time to demonstrate the presence of CTF dimers (lane 4, arrowhead 2); (3) a similar sample of purified LPHN1 was ^{125}I-iodinated, resolved by SDS-PAGE, and autoradiographed to visualize the major proteins present in a LPHN1 preparation (lane 6); (4) some of the ^{32}P- and ^{125}I-labeled samples were boiled to identify the CTF (lanes 2, 7). These additional data (including electrophoretic mobility, amount present in purified sample and susceptibility to boiling) allowed us to unequivocally identify the ^{32}P-phosphorylated bands present in purified LPHN1 (Fig. 2G, lane 1): the CTF-

19

b,c,d bands (filled arrowhead, CTF) and the CTF dimer (filled arrowhead, 2); in addition, a small amount of a 48-kDa CTF degradation fragment and an unidentified P93 protein (asterisk) were present. Surprisingly, CTF contained relatively little incorporated ^{32}P (compared to the P93 contaminant, which was only visible by ^{32}P autoradiography, but not by ^{125}I autoradiography). Based on the relative abundance of the ^{32}P-detected and immunostained CTF dimers (lanes 1 and 4, respectively), we estimated the proportion of slow migrating CTF monomers (CTF-b,c,d) that were phosphorylated. Thus, in the absence of exogenous stimulation of LPHN1, no more than 16.1 ± 4.6% of its CTF exchanges its phosphate groups within 1 h.

One unexpected observation from the above experiments was that the fast-migrating CTF-a band (or bands) in fact contained phosphate groups (on Tyr and Ser), but did not exchange them. This suggested that under the resting conditions, all or almost all LPHN1 CTF was phosphorylated and therefore this basal phosphorylation was unlikely to occur as a result of LPHN1 activation and subsequent desensitization. To support this hypothesis, we studied CTF phosphorylation in COS7 cells, which originate from kidney fibroblasts, do not demonstrate neuronal features and are unlikely to hyperactivate and desensitize LPHN1. These cells expressed LPHN1 well and partially cleaved it into NTF and CTF (Fig. 2H, lanes 3, 5). As these cells did not glycosylate the NTF very efficiently, both glycosylated and un-glycosylated NTF forms could be detected (open arrowheads). The cleaved CTF appeared as a single band of 65 kDa (black arrowhead). In addition, the cells accumulated the uncleaved, full-size LPHN1 (black arrow, LPHN1-FS), which is not normally delivered to the cell surface[7,33]. To test for CTF phosphorylation, we incubated COS7 cells expressing LPHN1 with [^{32}P]orthophosphate, overnight (Fig. 2H, lanes 1, 2). As a result, both the cleaved CTF and even the LPHN1-FS became phosphorylated (Fig. 2H, lane 1). In addition, a few other phosphorylated proteins were

detected (asterisks, lane 1), but they also appeared in cells transfected with an empty vector (asterisks, lane 2) and thus represented endogenous phosphorylated proteins. Thus, LPHN1 is spontaneously phosphorylated in both neuronal and non-neuronal cells, even before it is delivered to the cell surface, which supports the idea that at least its basal phosphorylation is not linked to its desensitization as a GPCR.

CTF phosphorylation map

To date, no experimental data about CTF phosphorylation in LPHN1 has been published. Therefore, we used several online resources to predict potential sites in the cytosolic loops and C-terminal tail of the CTF. From 30 to 50 potential phosphorylation sites were identified (Fig. 3A) as substrates for a large number of protein kinases: Ca^{2+}-calmodulin-dependent protein kinase II, caseine kinases 1 and 2, cyclin-dependent kinase 1 CDK1/CDK2, DNA-activated protein kinase, glycogen synthase kinase 3, insulin receptor – tyrosine kinase, p38 mitogen-activated protein kinase, protein kinase A, protein kinase C, protein kinase G, proto-oncogene tyrosine-protein kinase Src, and ribosomal s6 kinase. While some of these kinases are unlikely to phosphorylate LPHN1 because they localize in different cellular compartments (e.g. cdc2 is a nuclear protein, whereas LPHN1 is located in synapses), notably, no sites for GPCR kinases (GRKs), which are likely to phosphorylate LPHN1, were identified by any resource. In general, sequence-based phosphorylation site prediction appeared relatively unreliable: up to 30% of the phosphorylation sites assigned by different prediction tools did not coincide with each other, and most algorithms predicted some phosphorylation even in the NTF and extracellular loops of the CTF, which, while not entirely impossible, is highly unusual for a GPCR.

High-throughput tandem mass spectrometry (MS2), being based on phosphopeptide enrichment and peptide size determination, provides a somewhat more likely phosphorylation site assignment[36]. This method identifies 34 possible phosphorylation sites in the CTF (Fig. 3A). By only selecting those phosphorylation sites that have been predicted in more than 5 references[38–45], it is possible to limit the number of predicted phosphorylation sites to 7 most likely positions (Fig. 3B). The majority of these sites are located in the distal part of the C-terminal cytoplasmic tail, far from the cytosolic surface of the 7TMRs and are likely to affect CTF interactions with other proteins. Given this uncertainty about the number and positions of phosphorylated residues in the CTF, which made CTF mutagenesis approach inefficient, we decided to continue with pharmacological analysis of CTF phosphorylation.

α-LTX chromatography causes CTF dephosphorylation

To begin to understand the physiological role of CTF phosphorylation and to identify the enzymes involved in its regulation, we first analyzed how LPHN1 is distributed among sequentially purified brain membrane fractions[46]: (a) total brain homogenate (TB), (b) P1 pellet obtained by TB centrifugation (nuclei and broken cell bodies); (c) S1 supernatant obtained by TB centrifugation (post-nuclear membranes devoid of nuclei and neuronal cell bodies, but containing severed nerve terminals, fragments of axons, dendrites, mitochondria, somal vesicles, and somal cytosol), (d) P2 pellet obtained by S1 centrifugation (same as S1, but devoid of somal vesicles and cytosol); (e) synaptosomes purified from P2 by density gradient centrifugation (highly enriched nerve terminals containing small amounts of attached postsynaptic membrane; free from axonal and dendritic fragments), and (f) synaptic plasma membranes (SPM) obtained from synaptosomes by osmotic lysis (same as synaptosomes, but

free from presynaptic cytosol and vesicles). These membrane fractions were equalized for the amount of protein, separated by SDS-PAGE, and immunoblotted for both NTF and CTF. As demonstrated in Fig. 4A, both the NTF and CTF were present in all membrane fractions, except P1 (nuclei and cell bodies), but were strongly concentrated in synaptosomes and especially in SPM. Fractions discarded in the process of SPM purification (cell bodies, dendrites, axons) contained essentially no LPHN1 (Fig. 4A, P1; and not shown). This means that mature LPHN1 is a synaptic protein and should be a substrate for synaptic kinases and phosphatases.

These experiments led to an unexpected observation that the relative amounts of CTF bands differed among the membrane fractions. Thus, S1 contained a small proportion of the basally phosphorylated CTF-a, but a large amount of the fully phosphorylated CTF-d, while synaptosomes were rich in CTF-a, but had little CTF-d (Fig. 4A, B). This relationship remained when another detergent was used to solubilize the membranes (Fig. 4A, CHAPS), and thus did not depend on the efficiency of protein solubilization. This was puzzling, because all LPHN1 present in S1 came from the SPM compartment, so theoretically the staining in S1 should have been the same as in SPM. These results suggested that differential dephosphorylation of CTF occurred after sample solubilization and that it could be mediated by different phosphatases present in distinct membrane fractions. Indeed, when the membranes were solubilized in the presence of exogenous PPIs, the CTF bands appeared the same in all fractions (Fig. 4C). This result suggested that during the solubilization of synaptosomes and SPM, some CTF was dephosphorylated and converted to CTF-a, which did not happen upon S1 solubilization.

These findings called for a careful analysis of how the membranes affect CTF phosphorylation. To study LPHN1 fragments, we purified them from different membrane fractions using an α-

23

LTX affinity column[2], as shown above (Figs. 1, 2). While α-LTX only binds NTF[7], the CTF co-purifies with it, because the two fragments strongly interact via the N-terminal peptide of the CTF (*Stachel* peptide)[7,11]. Both the NTF and CTF always co-purified from S1 (Fig. 4D). However, surprisingly, practically no CTF was isolated with the NTF from synaptosomes and SPM (Fig. 4D). On average, only 10% of CTF was co-purified with the NTF from synaptosomes and SPM compared to S1 (Fig. 4E). Furthermore, the CTF from synaptosomes and SPM was largely dephosphorylated (Fig. 4D, Syn, SPM). As the starting membranes (S1, synaptosomes and SPM) contained similar amounts of CTF, which was also similarly phosphorylated (Fig. 4C), this dephosphorylation and loss of CTF could only be explained by the effect of α-LTX chromatography.

To ascertain that CTF dephosphorylation occurred during affinity chromatography, we carried out LPHN1 isolation in the presence of exogenous PPIs. As expected, this prevented CTF dephosphorylation (Fig. 4F). Surprisingly, the presence of PPIs also prevented the loss of CTF from the column, and LPHN1 purified from Syn, SPM and S1 contained the same amount of CTF (Fig. 4F). We hypothesized that CTF dephosphorylation leads to its loss. To demonstrate this, we carried out LPHN1 isolation from solubilized S1 membranes treated with alkaline phosphatase. Under these conditions, almost no CTF was co-purified with the NTF from S1 (Fig. 4G), similar to synaptosomes and SPM. This confirmed that the dephosphorylated CTF was lost during affinity chromatography.

We then asked whether this effect was caused specifically by affinity chromatography on α-LTX or any other protein that can bind LPHN1. When affinity chromatography of solubilized

synaptosomes was carried out using WGA as an adsorbent, no dephosphorylation or loss of CTF was observed (Fig. 4H).

This meant that α-LTX attached to the chromatography column either caused CTF dephosphorylation by itself or exposed CTF to another component that was also able to bind α-LTX. This idea was tested by varying the relative amounts of the α-LTX column and the solubilized membranes loaded onto it (termed here "differential load affinity chromatography"). The rational was that if a α-LTX-column was overloaded with LPHN1, then it would not have the capacity to bind any other proteins that interact with toxin weaker than LPHN1. Reciprocally, if a large excess of α-LTX-column was used, it would provide sufficient binding sites not only for LPHN1, but also for any protein/s that could mediate CTF dephosphorylation. However, if α-LTX itself was responsible for CTF dephosphorylation, by direct contact with LPHN1, then under both conditions all CTF would be equally dephosphorylated (and lost). When such experiments were conducted, the results (quantified in Fig. 4I, examples shown in Fig. 5A) demonstrated that using a large LTX column (">LTX") led to much deeper CTF dephosphorylation than overloading a LTX column with LPHN1 (">LPH"). This directly suggested that during affinity chromatography the excess of α-LTX on a large column provided binding sites for some phosphatase/s, which thus came into contact with the CTF and caused its dephosphorylation. In fact, at least one phosphatase, RPTPσ, is known to interact with LTX[47]. A direct experiment demonstrated that RPTPσ was indeed co-purified with LPHN1 on large LTX columns, but not on small LTX columns overloaded with LPHN1 (Fig. 4J).

Thus, considered together, our results indicated that the CTF of LPHN1 was dephosphorylated during the incubation with α-LTX and that this reaction was mediated by brain phosphatases

(in particular RPTPσ) recruited to LPNH1 by α-LTX, but not by WGA. The differential dephosphorylation of the CTF by various fractions of brain membranes suggested that they might contain distinct sets of endogenous phosphatases and endogenous PPIs, which would differentially affect the CTF during chromatography (see also Discussion).

Dephosphorylated CTF has a low affinity for the NTF

The results described above could explain CTF dephosphorylation during α-LTX affinity chromatography, but not its loss from column eluates. Several processes could lead to the disappearance of dephosphorylated CTF: (1) the loss of phosphate groups could destabilize the CTF and facilitate its proteolytic degradation; (2) it could irreversibly aggregate; or (3) it could be eluted from the column in earlier fractions.

As demonstrated above (Figs. 2D, E), dephosphorylation did not increase CTF degradation, but did cause some CTF aggregation. Although we could not exclude aggregation as one of the reasons behind the apparent loss of CTF, the aggregation never involved as much monomeric CTF as was lost in experiments with synaptosomes and SPM (compare Figs. 2B, D with Figs. 4D, G); in addition, treating α-LTX columns with SDS did not elute any aggregated CTF. Therefore, we carefully tested all fractions obtained during α-LTX-chromatography of solubilized synaptosomes, using the differential load affinity chromatography approach, as described in the previous section (Figs. 4I, J). When the amount of LTX on the column exceeded the amount of loaded LPHN1, we observed substantial dephosphorylation of CTF after overnight incubation (Fig. 5A, >LTX). Importantly, a large amount of CTF-a produced by dephosphorylation in this experiment appeared in the wash, where NTF was absent (Fig. 5A, >LTX). In contrast, when the loaded LPHN1 exceeded LTX on the column, no CTF

dephosphorylation, nor loss, occurred (Fig. 5A, >LPH). Quantification of these data (Fig. 5B), demonstrated a large and statistically highly significant loss of CTF from the final eluate under the LTX excess condition, compared to the LPH excess condition (Fig. 5B, Eluate). On the other hand, when the amount of CTF present in all fractions (including 0.5 M NaCl washes) was combined, no significant difference between the two conditions was observed (Fig. 5B, All fractions). These results showed that when the CTF was dephosphorylated on an α-LTX column, a large proportion of it dissociated from the NTF, while the latter remained bound to α-LTX.

The release of dephosphorylated CTF could be caused by (1) a weaker interaction between the NTF and dephosphorylated CTF or (2) a conformational change induced by α-LTX in the NTF that repelled the CTF. In addition, a direct role of α-LTX in CTF dephosphorylation was not entirely excluded by our differential load experiments above (Figs. 4I, J; 5A). One way to test all these possibilities was to separate purified LPHN1 on a different affinity column, for example WGA. This lectin binds the NTF of LPHN1, but does not cause receptor activation or separation of its fragments[9], like α-LTX does. On the other hand, WGA does not interact with the CTF, which is not glycosylated (Fig. 2A). For this experiment (schematically shown in Fig. 5C), we used LPHN1 purified on an α-LTX-column, which had been overloaded with S1 in the presence of exogenous PPIs to avoid any possible CTF dephosphorylation. This sample was then separated under three different conditions (Fig. 5C): (1) WGA-affinity chromatography of LPHN1 without any further treatment; (2) WGA-chromatography of LPHN1 treated with alkaline phosphatase to mimic CTF dephosphorylation on a column; and (3) second α-LTX affinity chromatography of untreated LPHN1. Using the eluate from a LTX column (Fig. 5C, D) had an additional advantage that it was devoid of any cellular protein phosphatases. In experiment 1,

both the NTF and all phosphorylated forms of CTF co-purified in the SDS eluate (Fig. 5E, Eluate). No CTF dephosphorylation occurred on this column and no CTF was present in wash fractions (Fig. 5E, Wash). When the receptor had been treated with alkaline phosphatase (experiment 2), both the NTF and CTF-a were seen binding to WGA-column, but about 90% of the CTF was then gradually released from the column by successive 0.5 M NaCl washes (Fig. 5F, Wash). Only about 10% of the original CTF-a remained attached to the NTF and was eluted by SDS (Fig. 5F, Eluate). In experiment 3, the purified LPHN1 did not become dephosphorylated on a second α-LTX-column and was isolated without losses (Fig. 5G).

These data indicated that CTF dephosphorylation during its purification from synaptic membranes (e.g. Fig. 4D, G, J) was mediated by cellular protein phosphatases rather than by a ligand (α-LTX or WGA) attaching to the NTF. Also, dephosphorylation of CTF apparently made the NTF-CTF complex less stable, leading to CTF release from the NTF by high salt washes. Finally, given the result in Fig. 5G, α-LTX binding to the NTF did not itself induce the release of phosphorylated CTF.

However, the problem with these data was that they were based on NTF binding to a column. Although the column material seemed to have no direct effect on CTF dephosphorylation or loss, it was still possible that the specific configuration of the NTF-CTF complex attached to a column could artificially affect its stability. To test this hypothesis, we used an opposite approach and assessed NTF-CTF complex stability by attaching it to an adsorbent via the CTF. For this purpose, we used anti-CTF antibodies bound to a protein A column to pull down the CTF. The CTF was either intact or treated with alkaline phosphatase. We then measured co-precipitation of the NTF with the CTF (Fig. 5H). The results of this experiment are shown in

Figs. 5I, J, where it can be seen that dephosphorylated CTF pulled down much less NTF than the fully phosphorylated control CTF. Thus, the stability of the NTF-CTF complex depends on the state of CTF phosphorylation and not on the manner in which it is pulled down.

CTF dephosphorylation in tissues and cells

These *in vitro* studies led to an important question whether ligand binding to the NTF could also affect CTF dephosphorylation in cells/tissues. We, therefore, compared αLTX-induced CTF phosphorylation and dephosphorylation in synaptosomes and neuroblastoma NB2a cells stably expressing LPHN1. The treatment of synaptosomes with 5 nM α-LTX for 1 h led to deep dephosphorylation of CTF (Fig. 6A). When LPHN1 was expressed in NB2a cells, its CTF migrated on SDS-gel as a series of bands resembling the basally phosphorylated CTF-a band and some highly phosphorylated CTF-b,c,d bands (Fig. 6B, bracket). To prove that this migration pattern reflected CTF phosphorylation, LPHN1 was isolated from NB2a cells using α-LTX chromatography and treated with alkaline phosphatase. As demonstrated in Fig. 6B, left, dephosphorylation clearly removed the slower migrating CTF bands and also caused some CTF dimer formation. When these NB2a cells were treated with 5 nM α-LTX for 1 h, the amount of CTF-d slightly decreased, while CTF-a increased, and a small amount of dimer formation was detected. However, the treatment of the cells with a high α-LTX concentration (30 nM) led to strong dephosphorylation of the CTF and formation of a significant amount of SDS-resistant complexes (CTF dimers and trimers) (Fig. 6B, arrowheads 2, 3).

These results indicated that α-LTX binding to the NTF could induce CTF dephosphorylation and dimerization by acting across the plasma membrane of living cells. Thus, the toxin could only cause CTF dephosphorylation if it recruited a phosphatase to the α-LTX-LPHN1 complex.

As was shown above (Fig. 4J), RPTPσ, which binds α-LTX, is one of the phosphatases that could participate in this reaction. We therefore analyzed the level of RPTPσ mRNA in the NB2a cells expressing LPHN1 (Fig. 6C). The amount of RPTPσ transcript was normalized to the mRNA level of β-actin, a housekeeping protein frequently used as a reference, and compared to the expression of two important proteins, stromal interacting molecules (STIM1 and 2), that are expressed in essentially all cells and participate in Ca^{2+} homeostasis. The level of RPTPσ mRNA exceeded that for STIM1 and 2 by a factor of 2 (Fig. 6D), suggesting that this phosphatase was actively produced by the neuroblastoma cells and could indeed mediate the effect of α-LTX on CTF dephosphorylation.

To test whether the basally phosphorylated CTF-a had a low affinity for the NTF not only *in vitro*, but also *in vivo*, and to avoid any direct effect of α-LTX on the NTF, we separated solubilized brain membranes (S1) by sucrose density gradient centrifugation. This method also allowed an estimation of the molecular size and stoichiometry of the NTF-CTF complexes (Fig. 6E, F). To calibrate the gradients and compare receptor preparations after different treatments, we also centrifuged several marker proteins (Fig. 6D) and SDS-denatured receptor (Fig. 6E, F, bottom panels).

We found that in untreated membrane samples, the distribution of the NTF paralleled that of the phosphorylated CTF-b,c,d bands, demonstrating mostly stoichiometric dimeric complexes (LPH*2) (370 kDa) and also some tetramers (LPH*4) (740 kDa), but almost no monomers (185 kDa) (Fig. 6E, F, top panels). This suggested that the phosphorylated forms of the CTF interacted with the NTF. However, most significantly, the basally phosphorylated CTF-a form trailed behind the NTF/CTF complexes (Fig. 6E; top panel, arrow). The position of the CTF-a

on the gradient indicated that it was dimeric, but there was no NTF in these fractions (Fig. 6F, insets).

When the native NTF-CTF complexes were centrifuged in the presence of an excess of α-LTX (Fig. 6E, F, middle panel, grey line), the NTF and CTF shifted to a denser region of the gradient, with molecular masses of 630 kDa and above, corresponding to a complex of LPHN1 dimers with LTX dimers (LPH*2-LTX*2) (Fig. 6E, F). Importantly, some amount of dephosphorylated CTF-a trailed in the lighter gradient fractions, suggesting that, due to a lack of NTF, it did not participate in α-LTX-induced NTF-CTF complex. These data indicate that LPHN1 is dimeric in neuronal membranes and contains almost only the phosphorylated CTF-b,c,d bands. The basally phosphorylated/dephosphorylated CTF-a appears to form dimeric complexes that lack NTF.

Discussion

Based on technical improvements in electrophoretic separation of spontaneously aggregating CTF (Fig. 1) and on the use of alkaline phosphatase with or without PPIs (Fig. 2), we show here, for the first time, that the CTF of LPHN1 is post-translationally modified by both reversible phosphorylation and possibly palmitoylation (Fig. 2). Possible phosphorylation of LPHN1 has been previously mentioned in several reviews[48–50], including a very comprehensive literature analysis[51], but, to our knowledge, never experimentally addressed (except using MS2-based predictions, see below). However, phosphorylation of GPCRs is very important for their functions[26,51] and, therefore, deserves an in-depth investigation. Many of the findings made in this paper will be directly applicable to other Adhesion GPCRs.

Theoretical predictions suggest that CTF of LPHN1 can be phosphorylated on ~ 50 sites that can serve as substrates for various kinases. Based on high-throughput MS2, 34 peptides have been identified as potentially phosphorylated and tentatively assigned to LPHN1[36] (Fig. 3A), with 5 potential sites in the *cytosolic loops 2* and *3*, and a large number in the C-terminal tail. Of the 34 potentially phosphorylated peptides, 7 sequences have been identified between 5 and 86 times, suggesting that they are likely to be present in the CTF of LPHN1. However, it must be stressed that the MS2 assignment is still probabilistic, and none of these 34 peptides has been confirmed by sequence analysis. Four of the 7 most frequently hit peptides are not recognized as likely phosphorylation sites by any consensus sequence prediction algorithms, and the MS2 method regularly predicts multiple phosphorylation sites in the extracellular domains of LPHN1. Our experimental data agree with a relatively low number of phosphorylation sites, which involve Tyr, Ser, and Thr and appears as 4 protein bands that have different mobilities on the SDS-gels (Fig. 1A; 2F). This suggests that 7-10 phosphate groups can be attached to the slow-migrating CTF-d. This multi-site phosphorylation resembles the "barcode" type of phosphorylation by GRKs observed in many GPCRs[26,52]. Given the large number of potential phosphorylation sites in LPHN1, experimental analysis of its CTF phosphorylation is now required.

What could be the functional role of this phosphorylation? The most interesting feature of CTF phosphorylation is that it leads to a change in CTF affinity for the NTF (Fig. 4-6): the phosphorylated CTF binds the NTF much stronger than the basally phosphorylated or dephosphorylated CTF. CTF phosphorylation in the brain, where LPHN1 expression by far exceeds its expression in any other tissues, apparently occurs prior to its normal function in synapses. Indeed, CTF is phosphorylated when LPHN1 is transiently expressed in COS and

NB2a cells (Figs. 2H, 6B), even before the protein is cleaved and delivered to the cell surface (Fig. 2H).

In a vast number of receptors, ligand-induced phosphorylation, especially by GRKs, is associated with a decrease in ligand affinity, increased receptor desensitization and internalization[27,53–56]. However, LPHN1 (as an Adhesion GPCR) is unusual because it consists of two fragments, of which the NTF is engaged in strong cell-surface interactions with other proteins across the synaptic cleft[12,57]. Unless the NTF is proteolytically cleaved, its internalization is not possible. As phosphorylated CTF binds strongly to the NTF, it would also be unable to internalize. In addition, the CTF and the whole LPHN1 are unlikely to undergo the lysosomal pathway of internalization, because this would lead to their retrograde transport to neuronal somata[58,59], and LPHN1 fragments are not observed in the P1 (Fig. 4A) or cytosolic vesicular fractions (not shown). Therefore, CTF desensitization and recovery probably occur while it remains in the plasma membrane, without internalization. On the other hand, the recycling of phosphate groups in highly phosphorylated CTF species is slow, constituting no more than 16% per hour. (Fig. 2). Finally, given that up to 100% of LPHN1 in nerve terminals is variously phosphorylated, the phosphorylated CTF must be an active form of LPHN1 rather than desensitized and destined for recycling, as in the case of GRK-phosphorylated GPCRs.

On the other hand, similar to some other GPCRs[60], differently phosphorylated LPHN1 forms can have distinct activities. In fact, the binding of LTX[N4C], to the NTF causes NTF-CTF association and massive activation of the CTF[7]. The effect of LTX[N4C] can continue for hours in a burst-like manner, without showing any signs of desensitization[61]. However, activation by α-LTX also leads to CTF dephosphorylation by cellular protein phosphatases (Figs. 4D, E, G, J;

5A; 6A, B), including RPTPσ, in a process that is schematically presented in Fig. 7. As a result, CTF affinity for the NTF decreases and it can dissociate from the complex (Fig. 5A, F, I; 6E). This obviously should stop the signaling induced by α-LTX, which only interacts with the NTF. However, it is tempting to speculate that this separation leads to a change in signaling specificity of LPHN1. Indeed, when LTX[N4C] acts via the NTF-CTF complex, it clearly stimulates Gαq-mediated signaling via PLC to internal Ca^{2+} stores[20,62]. On the other hand, the CTF of LPHN1 expressed without the NTF demonstrates a different signaling specificity and (at least when it is stimulated by exogenous *Stachel* peptide) activates Gαi, leading to a decrease in cAMP levels[63]. Thus, the activation of one signaling pathway may cause the CTF to dissociate from the complex and switch to another signaling pathway, where the CTF could act as a non-Adhesion GPCR. In this process, the NTF would play the role of a molecular switch. CTF phosphorylation might also regulate its interaction with intracellular partners. Therefore, it is important to use phosphorylated forms of CTF when modeling its interaction with other proteins.

Based on our data, LPHN1 appears to be always phosphorylated in synaptic membranes and in transfected cells (Figs. 1A, 2A, H; 6B) and remains largely phosphorylated even after long incubation in detergent extracts (Fig. 4A). However, both nerve terminals and NB2a cells contain RPTPσ and other phosphatases, which could theoretically dephosphorylate LPHN1, especially in detergent lysates. The stability of CTF phosphorylation could be explained by an equilibrium between the activities of phosphatases and kinases. However, CTF exchanges phosphate groups rather slowly (Fig. 2G); in addition, dephosphorylation does not prevail even after overnight incubations in detergent lysate (e.g. Fig. 4H), when ATP required for phosphorylation should be gradually lost. Thus, constant phosphorylation and dephosphorylation of LPHN1 is unlikely. It is thus possible that synaptic phosphatases that

target LPHN1 are normally inhibited and only slightly dephosphorylate the CTF (Fig. 4A). Alternatively, LPHN1 may normally exist in a conformation that does not allow its dephosphorylation. In fact, when α-LTX is added to solubilized membranes (in Sepharose-immobilized form, Fig. 4D, G, J) or to synaptosomes and cells (in its soluble form, Fig. 6A, B), this leads to deep CTF dephosphorylation, possibly because α-LTX activates both LPHN1 and phosphatases, especially RPTPσ, which also binds α-LTX[47] (Fig. 4J). Given that WGA, which also binds LPHN1, does not cause LPHN1 dephosphorylation after overnight incubation (Fig. 4H), it is probable that LPHN1 dephosphorylation requires the activation of both LPHN1 and possibly phosphatase/s by an agonist (e.g. α-LTX).

The purified neuronal compartments that normally contain LPHN1 (synaptosomes and SPM) have active phosphatases that dephosphorylate LPHN1 either spontaneously (albeit weakly) (Fig. 2A) or after activation by α-LTX (Figs. 4, 5A). One peculiar observation made here is that when these neuronal compartments are "contaminated" with components of neuronal cell bodies (TB or S1 fractions), which themselves lack LPHN1 (Fig. 4A), this leads to a strong inhibition of CTF dephosphorylation, whether spontaneous or α-LTX-mediated (Fig. 4A, D). This suggests that endogenous PPIs (probably regulatory subunits of protein phosphatases) are more abundant in the TB or S1 fractions than any protein phosphatases in nerve terminals. These "contaminating" PPIs, present in the somal cytosol or fragments of the endoplasmic reticulum, could ectopically inhibit CTF dephosphorylation by synaptic phosphatases when they areactivated by solubilization or by α-LTX. On the other hand, PPIs present in synapses are unable to protect CTF from α-LTX-induced dephosphorylation, probably because α-LTX brings the CTF and RPTPσ (and other phosphatases) into close apposition. An interaction of α-LTX with its two receptors (RPTPσ and LPHN1) could be the mechanism by which α-LTX

dephosphorylates the CTF and so efficiently signals via LPHN1 (Fig. 7). However, given that CTF is phosphorylated not only on Tyr, but also Ser and Thr, it is clear that RPTPσ is not the only phosphatase targeting LPHN1.

Finally, as dephosphorylation weakens the CTF-NTF interaction (Figs. 4, 5), it is important to consider this hypothesis in light of the ability of LPHN1 fragments to dissociate and re-associate reversibly, as described previously[7,8] and later independently confirmed using another Adhesion GPCR[64]. This dissociation and especially association have been a contentious issue, especially considering the 3D structure of the LPHN1 GAIN domain[11], which demonstrates that the *Stachel* peptide is essentially buried in the C-terminal part of the NTF, making it hard to imagine how the two could separate, let alone reassemble afterwards. However, the dissociation-association was observed only on the cell surface and not when the NTF and CTF were expressed as soluble proteins[7,8,64]. It is possible that the anchoring mechanism, which holds the NTF on the membrane, also helps to maintain an open cavity within the GAIN domain, which allows the CTF docking/undocking. Alternatively, it is possible that the reassociation does not fully restore the tight grasp of the *Stachel* peptide by the GAIN domain[11]. The two LPHN1 fragments might interact in many different ways, but it is clear that α-LTX binding to the NTF leads to its reassembly with the CTF on the cell membrane, allowing LPHN1 to mediate an intracellular signal[7,8,64], and CTF dephosphorylation could be involved in generating this signal.

In conclusion, we propose that the strength of NTF-CTF interaction is based on the phosphorylation state of the CTF and this may affect the physiological functions of LPHN1. Previously, we described the dynamic nature of NTF-CTF interaction[7,8]. This paper reveals the first details of how this interaction may be regulated in cells. Other Adhesion GPCRs may be

subject to similar modulation, and it will be important to study these processes in other members of this family.

Acknowledgments

Competing interests

JPS is employed by UCB-Pharma. JS is employed by Thomsons Online Benefits. All other authors declare no competing interests.

YAU conceived and coordinated the study, analyzed the results and wrote the article. MAR, CM, OB, JS, JKB, and JPS designed, performed and analyzed the experiments. MAR and OB contributed to the manuscript. All authors were involved in revising the article and approved the final version of the manuscript.

References

1. Hamann J., G. Aust, D. Arac, *et al.* 2015. International Union of Basic and Clinical Pharmacology. XCIV. Adhesion G Protein-Coupled Receptors. *Pharmacol. Rev.* **67**: 338–367.

2. Davletov B.A., O.G. Shamotienko, V.G. Lelianova, *et al.* 1996. Isolation and biochemical characterization of a Ca2+-independent α-latrotoxin-binding protein. *J. Biol. Chem.* **271**: 23239–23245.

3. Krasnoperov V.G., R. Beavis, O.G. Chepurny, *et al.* 1996. The calcium-independent receptor of α-latrotoxin is not a neurexin. *Biochem. Biophys. Res. Commun.* **227**: 868–

875.

4.   Krasnoperov V.G., M.A. Bittner, R. Beavis, *et al.* 1997. α-Latrotoxin stimulates exocytosis by the interaction with a neuronal G-protein-coupled receptor. *Neuron* **18**: 925–937.

5.   Lelianova V.G., B.A. Davletov, A. Sterling, *et al.* 1997. α-Latrotoxin receptor, latrophilin, is a novel member of the secretin family of G protein-coupled receptors. *J. Biol. Chem.* **272**: 21504–21508.

6.   Lin H.H., G.W. Chang, J.Q. Davies, *et al.* 2004. Autocatalytic cleavage of the EMR2 receptor occurs at a conserved G protein-coupled receptor proteolytic site motif. *J. Biol. Chem.* **279**: 31823–31832.

7.   Volynski K.E., J.-P.P. Silva, V.G. Lelianova, *et al.* 2004. Latrophilin fragments behave as independent proteins that associate and signal on binding of LTXN4C. *EMBO J.* **23**: 4423–4433.

8.   Silva J.-P., V. Lelianova, C. Hopkins, *et al.* 2009. Functional cross-interaction of the fragments produced by the cleavage of distinct adhesion G-protein-coupled receptors. *J. Biol. Chem.* **284**: 6495–6506.

9.   Rahman M.A., A.C. Ashton, F.A. Meunier, *et al.* 1999. Norepinephrine exocytosis stimulated by α-latrotoxin requires both external and stored Ca2+ and is mediated by latrophilin, G proteins and phospholipase C. *Philos. Trans. R. Soc. B Biol. Sci.* **354**: 379–386.

10.   Krasnoperov V., Y. Lu, L. Buryanovsky, *et al.* 2002. Post-translational proteolytic processing of the calcium-independent receptor of α-latrotoxin (CIRL), a natural chimera of the cell adhesion protein and the G protein-coupled receptor: Role of the G protein-coupled receptor proteolysis site (GPS) motif. *J. Biol. Chem.* **277**: 46518–46526.

11.   Arac D., A.A. Boucard, M.F. Bolliger, *et al.* 2012. A novel evolutionarily conserved domain of cell-adhesion GPCRs mediates autoproteolysis. **31**: 1364–1378.

12.   Silva J.-P., V.G. Lelianova, Y.S. Ermolyuk, *et al.* 2011. Latrophilin 1 and its endogenous ligand Lasso/teneurin-2 form a high-affinity transsynaptic receptor pair with signaling capabilities. *Proc. Natl. Acad. Sci. U. S. A.* **108**: 12113–12118.

13.   O'Sullivan M.L., J. de Wit, J.N. Savas, *et al.* 2012. FLRT Proteins Are Endogenous Latrophilin Ligands and Regulate Excitatory Synapse Development. *Neuron* **73**: 903–910.

14.   Zuko A., A. Oguro-ando, H. Post, *et al.* 2016. Association of cell adhesion molecules contactin-6 and latrophilin-1 regulates neuronal apoptosis. **9**: Article 143 1-16.

15. Vysokov N. V, J.-P.P. Silva, V.G. Lelianova, *et al.* 2016. The mechanism of regulated release of Lasso/teneurin-2. *Front. Mol. Neurosci.* **9**: 59.

16. Vysokov N. V, J.-P. Silva, V.G. Lelianova, *et al.* 2018. Proteolytically released Lasso/teneurin-2 induces axonal attraction by interacting with latrophilin-1 on axonal growth cones. *Elife* **7**: pii: e3793.

17. Ushkaryov Y.A., A. Rohou & S. Sugita. 2008. α-Latrotoxin and its receptors. In *Pharmacology of Neurotransmitter Release* Sudhof T.C. & Starke K., Eds. 171–206. Berlin, Heidelberg: Springer-Verlag.

18. Orlova E. V, M.A. Rahman, B. Gowen, *et al.* 2000. Structure of α-latrotoxin oligomers reveals that divalent cation-dependent tetramers form membrane pores. *Nat. Struct. Biol.* **7**: 48–53.

19. Ichtchenko K., M. Khvotchev, N. Kiyatkin, *et al.* 1998. α-Latrotoxin action probed with recombinant toxin: Receptors recruit α-latrotoxin but do not transduce an exocytotic signal. *EMBO J.* **17**: 6188–6199.

20. Capogna M., K.E. Volynski, N.J. Emptage, *et al.* 2003. The alpha-latrotoxin mutant LTXN4C enhances spontaneous and evoked transmitter release in CA3 pyramidal neurons. *J. Neurosci.* **23**: 4044–53.

21. Volynski K.E., M. Capogna, A.C. Ashton, *et al.* 2003. Mutant α-latrotoxin (LTXN4C) does not form pores and causes secretion by receptor stimulation. This action does not require neurexins. *J. Biol. Chem.* **278**: 31058–31066.

22. Ashton A.C., K.E. Volynski, V.G. Lelianova, *et al.* 2001. α-Latrotoxin, Acting via Two Ca2+-dependent Pathways, Triggers Exocytosis of Two Pools of Synaptic Vesicles. *J. Biol. Chem.* **276**: 44695–44703.

23. Liu J., Q. Wan, X. Lin, *et al.* 2005. α-Latrotoxin modulates the secretory machinery via receptor-mediated activation of protein kinase C. *Traffic* **6**: 756–765.

24. Lajus S., P. Vacher, D. Huber, *et al.* 2006. α-Latrotoxin induces exocytosis by inhibition of voltage-dependent K+ channels and by stimulation of L-type Ca2+channels via latrophilin in β-cells. *J. Biol. Chem.* **281**: 5522–5531.

25. Lelyanova V.G., D. Thomson, R.R. Ribchester, *et al.* 2009. Activation of α-latrotoxin receptors in neuromuscular synapses leads to a prolonged splash acetylcholine release. *Bull. Exp. Biol. Med.* **147**: 701–703.

26. Butcher A.J., K.C. Kong, R. Prihandoko, *et al.* 2012. Physiological role of G-protein coupled receptor phosphorylation. In *Muscarinic Receptors* Fryer A.D., Christopoulos A., & Nathanson N.M., Eds. 79–94. London: Springer.

27. Gainetdinov R.R., R.T. Premont, L.M. Bohn, *et al.* 2004. Desensitization of G protein-coupled receptors and neuronal functions. *Annu. Rev. Neurosci.* **27**: 107–144.

28. Gurevich V. V & E. V Gurevich. 2019. GPCR signaling regulation : the role of GRKs and arrestins. *Front. Pharmacol.* **10**: 1–11.

29. Hilbig D., D. Sittig, F. Hoffmann, *et al.* 2018. Mechano-dependent phosphorylation of the PDZ-binding motif of CD97/ADGRE5 modulates cellular detachment. **24**: 1986–1995.

30. Davydov I.I.I., S. Fidalgo, S.A.A. Khaustova, *et al.* 2009. Prediction of epitopes in closely related proteins using a new algorithm. *Bull. Exp. Biol. Med.* **148**: 869–873.

31. Volynski K.E., F.A. Meunier, V.G. Lelianova, *et al.* 2000. Latrophilin, neurexin, and their signaling-deficient mutants facilitate α-latrotoxin insertion into membranes but are not involved in pore formation. *J. Biol. Chem.* **275**: 41175–41183.

32. Gordon-Weeks P.R. 1997. Isolation of synaptosomes, growth cones and their subcellular components. In *Neurochemistry. A Practical Approach* Turner A.J. & Bachelard H.S., Eds. 1–26. Oxford, UK: IRL Press.

33. Ashton A.C., M.A. Rahman, K.E. Volynski, *et al.* 2000. Tetramerisation of α-latrotoxin by divalent cations is responsible for toxin-induced non-vesicular release and contributes to the Ca2+-dependent vesicular exocytosis from synaptosomes. *Biochimie* **82**: 453–468.

34. Petrenko A.G., V.D. Lazaryeva, M. Geppert, *et al.* 1993. Polypeptide composition of the α-latrotoxin receptor. High affinity binding protein consists of a family of related high molecular weight polypeptides complexed to a low molecular weight protein. *J. Biol. Chem.* **268**: 1860–7.

35. Laemmli U.K. 1970. Cleavage of structural proteins during the assembly of the head of bacteriophage T4. *Nature* **227**: 680–685.

36. Hornbeck P. V, J.M. Kornhauser, V. Latham, *et al.* 2019. 15 years of PhosphoSitePlus®: integrating post-translationally modified sites , disease variants and isoforms. *Nucleic Acids Res.* **47**: 433–441.

37. Ruijter J.M., C. Ramakers, W.M.H. Hoogaars, *et al.* 2009. Amplification efficiency: linking baseline and bias in the analysis of quantitative PCR data. **37**: e45 1-12.

38. Lundby A., A. Secher, K. Lage, *et al.* 2012. Quantitative maps of protein phosphorylation sites across 14 different rat organs and tissues. *Nat. Commun.* **3**: 810–876.

39. Sacco F., S.J. Humphrey, M. Mischnik, *et al.* 2016. Glucose-regulated and drug-

perturbed phosphoproteome reveals molecular mechanisms controlling insulin secretion. *Nat. Commun.* **7**: 13250.

40. Kettenbach A.N., D.K. Schweppe, B.K. Faherty, *et al.* 2013. Quantitative phosphoproteomics identifies substrates and functional modules of aurora and polo-like kinase activities in mitotic cells. **4**: rs5.

41. Palacios-Moreno J., L. Foltz, A. Guo, *et al.* 2015. Neuroblastoma tyrosine kinase signaling networks involve FYN and LYN in endosomes and lipid rafts. **11**: e1004130 1-33.

42. Ding V.M.Y., P.J. Boersema, L.Y. Foong, *et al.* 2011. Tyrosine phosphorylation profiling in FGF-2 stimulated human embryonic stem cells. **6**: e17538.

43. Moritz A., Y. Li, A. Guo, *et al.* 2011. Akt-RSK-S6 kinase signaling networks activated by oncogenic receptor tyrosine kinases. **3**: ra64.

44. Jørgensen C., A. Sherman, G.I. Chen, *et al.* 2014. Cell-specific information processing in segregating populations of Eph receptor ephrin-expressing cells. **326**: 1502–1509.

45. Brill L.M., A.R. Salomon, S.B. Ficarro, *et al.* 2004. Robust phosphoproteomic profiling of tyrosine phosphorylation sites from human T cells using immobilized metal affinity chromatography and tandem mass spectrometry. **76**: 2883–2892.

46. Berninghausen O., M.A. Rahman, J.-P.P. Silva, *et al.* 2007. Neurexin Iβ and neuroligin are localized on opposite membranes in mature central synapses. *J. Neurochem.* **103**: 1855–1863.

47. Krasnoperov V., M.A. Bittner, W. Mo, *et al.* 2002. Protein-tyrosine phosphatase-σ is a novel member of the functional family of α-latrotoxin receptors. **277**: 35887–35895.

48. Silva J.-P., J. Suckling & Y. Ushkaryov. 2009. Penelope's web: Using α-latrotoxin to untangle the mysteries of exocytosis. *J. Neurochem.* **111**: 275–290.

49. Meza-Aguilar D.G. & A.A. Boucard. 2014. Latrophilins updated. *BioMol Concepts* **5**: 457–478.

50. Silva J.-P. & Y. Ushkaryov. 2010. The latrophilins, "split-personality" receptors. In *Adhesion-GPCRs: Structure to Function* Yona S. & Stacey M., Eds. 59–75. Austin: Landes Boscience & Springer Science + Business Media.

51. Langenhan T., G. Aust & J. Hamann. 2013. Sticky signaling — Adhesion Class G Protein-coupled Receptors take the stage. **6**: re3 1-22.

52. Yang Z., F. Yang, D. Zhang, *et al.* 2017. Phosphorylation of G protein-coupled receptors: from the barcode hypothesis to the flute model. *Mol. Pharmacol.* **92**: 201–

210.

53.   Carman V. & J.L. Benovic. 1998. G-protein-coupled receptors: turn-ons and turn-offs. *Curr. Opin. Neurobiol.* **8**: 335–344.

54.   Holtmann M.H., B.F. Roettger, D.I. Pinon, *et al.* 1996. Role of receptor phosphorylation in desensitization and internalization of the secretin receptor. *J. Biol. Chem.* **271**: 23566–23571.

55.   Pitcher J.A., N.J. Freedman & R.J. Lefkowitz. 1998. G protein – coupled receptor kinases. *Annu. Rev. Biochem.* **67**: 633–692.

56.   Marchese A., M.M. Paing, B.R.S. Temple, *et al.* 2008. G protein-coupled receptor sorting to endosomes and lysosomes. *Annu. Rev. Pharmacol. Toxicol.* **48**: 601–629.

57.   Boucard A.A., S. Maxeiner & T.C. Südhof. 2014. Latrophilins function as heterophilic cell-adhesion molecules by binding to teneurins: Regulation by alternative splicing. *J. Biol. Chem.* **289**: 387–402.

58.   Ferguson S.S.G. & M.G. Caron. 1998. G protein-coupled receptor adaptation mechanisms. *Cell Devel. Biol.* **9**: 119–127.

59.   Vukoja A., U. Rey, A.G. Petzoldt, *et al.* 2018. Presynaptic biogenesis requires axonal transport of lysosome-related vesicles. *Neuron* **99**: 1216-1232.e7.

60.   Daaka Y., L.M. Luttrell & R.J. Lefkowitz. 1997. Switching of the coupling of the β2-adrenergic receptor to different G proteins by protein kinase A. *Nature* **390**: 88–91.

61.   Lelyanova V.G., D. Thomson, R.R. Ribchester, *et al.* 2009. Activation of α-latrotoxin receptors in neuromuscular synapses leads to a prolonged splash acetylcholine release. *Bull. Exp. Biol. Med.* **147**: 701–3.

62.   Davletov B.A., F.A. Meunier, A.C. Ashton, *et al.* 1998. Vesicle exocytosis stimulated by α-latrotoxin is mediated by latrophilin and requires both external and stored Ca2+. *EMBO J.* **17**: 3909–3920.

63.   Nazarko O., A. Kibrom, J. Winkler, *et al.* 2018. A comprehensive mutagenesis screen of the Adhesion GPCR latrophilin-1/ADGRL1. *iScience* **3**: 264–278.

64.   Huang Y.-S., N.-Y. Chiang, C.-H. Hu, *et al.* 2012. Activation of myeloid cell-specific adhesion class G protein-coupled receptor EMR2 via ligation-induced translocation and interaction of receptor subunits in lipid raft microdomains. *Mol. Cell. Biol.* **32**: 1408–1420.

Figure legends

Figure 1. Analysis of the CTF of LPHN1 by SDS-PAGE. A. LPHN1 isolated on an α-LTX column from rat brain S1 membranes was separated in an 8% SDS-gel (conditions indicated at the top), and immunoblotted with antibodies against the NTF or CTF (shown at the bottom). Inset, electrophoretic separation of the CTF into 4 bands. **B.** Computer-aided densitometry of the CTF bands. Black line, an average profile; blue bars, standard deviation. **C.** Immunoblotting of brain membranes from wild-type and LPHN1 knockout (KO) mice for neurexin Iα (NRXN1), NTF and CTF. Arrowhead shows a lack of CTF staining in the KO brain. The numbers of independent experiments (*n*) were: A, 5; B, 6; C, 4.

Figure 2. The CTF of LPHN1 is phosphorylated on several sites. A. LPHN1 purified from S1 rat brain membranes on α-LTX was treated with neuraminidase and PNGase F or O-glycosidase, separated by SDS-PAGE and immunoblotted using affinity-purified antibodies against NTF and/or CTF. Inset, extended SDS-PAGE of LPHN1 in a 4% SDS-gel, immunoblotted for NTF. **B.** α-LTX-purified LPHN1 (left) or crude S1 membranes (right) were incubated with alkaline phosphatase (AP), in the absence or presence of exogenous PPIs. **C.** Computer-aided densitometry of the purified LPHN1 before (control) and after (AP) treatment with alkaline phosphatase. **D.** LPHN1 purified or from rat S1 membranes was treated with increasing doses of AP and hydroxylamine in the order shown. Right, a larger image of the blots showing lanes 2 and 3 to demonstrate that dephosphorylation of CTF induced its aggregation, but not degradation. Detergent extract from COS7 cells transiently transfected with LPHN1 was used as a marker of the dephosphorylated CTF. **E.** Quantification of all CTF-stained monomers and aggregates before (No AP) and after (AP) treatment with alkaline phosphatase. **F.** Purified LPHN1 treated ($^+$) or untreated (–) with alkaline phosphatase was immunoblotted with antibodies against phosphorylated amino acids. **G.** Lanes 1, 2: synaptosomes (Syn) were incubated with ^{32}P orthophosphate, solubilized and used to isolate LPHN1, which was separated by SDS-PAGE, transferred onto PVDF membrane and autoradiographed for 40 h. Lanes 3-5: the same blot as in lane 1 was immunostained for CTF and NTF; lane 4, long exposure. Lanes 6, 7: for comparison, purified LPHN1 was labeled with

[125]I, blotted and autoradiographed for 16 h. Lanes 2, 7: the electrophoretic samples were boiled for 5 min before loading on SDS-gels. Filled arrowheads, CTF and CTF dimer (2); open arrowhead, NTF; asterisk, a phosphorylated contaminant; arrow, aggregated CTF at gel top (Aggr.). **H.** COS7 cells transiently expressing LPHN1 (or empty vector) were [^{32}P]-phosphorylated, separated by SDS-PAGE, transferred onto membrane and exposed to an X-ray film for 24 h (lanes 1, 2). The membrane was then immunostained for NTF and CTF (lanes 3-6). ^{32}P-labeled cellular proteins in control and LPHN1 cells are marked by asterisks. The immunoblot shows the uncleaved full-size LPHN1 (FS, black arrow), glycosylated (glyc.) and unglycosylated (unglyc.) NTF (open arrowheads) and the single CTF band (black arrowhead). Note that both the single CTF band and the FS LPHN1 are phosphorylated. The numbers of independent experiments (*n*) were: A, 4; B, 8/12; C, 8/12; D, 8; E, 8; F, 3; G, 3; H, 3.

Figure 3. A map of predicted phosphorylation sites in the CTF. A. Phosphorylation sites predicted by high-throughput MS2[36] are indicated by circles, with the bar height proportional to the number of potential hits and the red color denoting sites with more than 5 hits. **B.** The positions and surrounding peptide sequences of the seven potentially phosphorylated residues (red circles in A); the predicted phosphorylated residues are encircled. The table also shows the number of theoretical hits and selected references reporting the predictions.

Figure 4. The CTF is dephosphorylated by cytosolic protein phosphatases and is lost from NTF. A. Brain membrane fractions (P1; S1; synaptosomes, Syn; and SPM) were solubilized in Thesit or CHAPS (for comparison of solubilization efficiency) and immunoblotted for NTF and CTF. LPHN1 expressed in COS7 cells was used as a marker of NTF and CTF proteins (labeling as in Fig. 2H). **B.** Differential abundance of the basally phosphorylated CTF-a (left) and maximally phosphorylated CTF-d (right) in respective brain membranes. t-Test with Bonferroni correction: *, p < 0.05. **C.** Inhibition of differential CTF dephosphorylation in the same membrane fractions by exogenous PPIs. **D.** CTF co-purifies with NTF on α-LTX columns from S1, but not from synaptosomes or SPM (two independent experiments with different exposure are shown). **E.** Quantification of CTF co-purifying with NTF on α-LTX-columns from respective membrane fractions. **F.** In the presence of exogenous PPIs, CTF co-purifies with NTF on α-LTX columns from all membranes. **G.** Alkaline phosphatase-induced dephosphorylation of CTF in S1 blocks its co-purification with NTF. H. The CTF in solubilized synaptosomes is not

dephosphorylated and co-purifies with NTF on WGA-columns. **I.** Quantification of differential load affinity chromatography (example shown in Fig. 5A), in which the α-LTX column is either overloaded with an excess of LPHN1 in solubilized S1 membranes (>LPH) or is in excess over solubilized S1 (>LTX). t-Test with Bonferroni correction: ***, p < 0.001. **J.** Differential load α-LTX-affinity chromatography with solubilized synaptosomes; the eluates are immunoblotted for NTF, CTF, and RPTPσ. The numbers of independent experiments (*n*) were: A, 3; B, 3; C, 6; D, 5; E, 5; F, 6; G, 3; H, 3; I, 5; J, 3.

Figure 5. The CTF dephosphorylation decreases its high affinity for the NTF. A. Differential load α-LTX-affinity chromatography of solubilized synaptosomes. CTF is dephosphorylated during chromatography under >LTX condition and is released from the column in wash fractions. Overloading α-LTX-columns with LPHN1 in solubilized membranes blocks CTF dephosphorylation and dissociation from NTF. **B.** Quantification of differentia load α-LTX-affinity chromatography experiments, as in A. t-Test with Bonferroni correction: **, p < 0.01; ***, p < 0.001. **C.** A scheme of experiments with secondary affinity chromatography of purified LPHN1 on α-LTX or WGA-columns, with or without alkaline phosphatase treatment. **D – G.** LPHN1 purified on α-LTX from S1 membranes was chromatographed on a WGA-column (with or without alkaline phosphatase, AP) or on an α-LTX column. **E, F.** WGA-chromatography of purified LPHN1 in the absence (**E**) or in the presence (**F**) of AP. **G.** Secondary chromatography of purified LPHN1 on an α-LTX column, in the absence of AP. Note that CTF is not dephosphorylated in the absence of other synaptosomal proteins. **H.** A scheme of immunoprecipitation experiments with LPHN1 purified from solubilized S1, with or without treatment with alkaline phosphatase, as shown in I. **I.** LPHN1 purified from S1 on an α-LTX-column was treated with or without alkaline phosphatase and immunoprecipitated using chicken anti-CTF antibodies and immunoblotted for CTF and NTF using respective rabbit antibodies. **J.** Quantification of experiments, as in I. The NTF yield in control experiments (No AP) taken as 100%. t-Test: **, p < 0.01. The numbers of independent experiments (*n*) were: A, 5; B, 5; D, 21; E, 3; F, 3; G, 3; I, 5; J, 5.

Figure 6. CTF dephosphorylation in cells and tissues. A. Synaptosomes were treated with 5 nM α-LTX for 1 h with oxygenation, then solubilized, separated by SDS-PAGE and immunoblotted for α-LTX, NTF and CTF. **B.** Left: LPHN1 purified from transfected NB2a cells

was treated with alkaline phosphatase, separated by SDS-PAGE and immunoblotted for NTF and CTF. The CTF is phosphorylated, showing several differently migrating bands, which disappear on AP treatment. Right: LPHN1-expressing NB2a cells were incubated for 1 h with increasing amounts of α-LTX. α-LTX causes LPHN dephosphorylation and dimerization. **C.** RT-PCR analysis of RPTPσ mRNA in LPHN1-expressing NB2a cells. β-Actin mRNA was used for normalization, STIM1 and STIM2 used for comparison. **D.** Calibration curve for sucrose density gradients, as shown in E, using molecular mass marker proteins: thyroglobulin, apoferritin, β-amylase, α-LTX, aldolase, BSA. **E.** Rat brain membranes (S1) were solubilized in Thesit and centrifuged in sucrose density gradients, as described under Methods. The gradient fractions were separated by SDS-PAGE and immunoblotted for α-LTX (middle panel), NTF and CTF (3 gels were used to separate each gradient). Top, untreated solubilized S1 membranes. Middle, solubilized S1 membranes centrifuged in the presence of a large excess of α-LTX. Bottom, solubilized S1 membranes centrifuged after treatment with 1% SDS and 100 mM DTT. **F.** Quantification of NTF and CTF distribution in gradient fractions (from E). Insets, LPHN1 at the bottom and top of gradient contains differentially phosphorylated CTF; only CTF is present in the top gradient fractions. The positions of predicted molecular species are shown at the top; the positions of molecular mass markers are shown in the bottom graph. The numbers of independent experiments (*n*) were: A, 4; B, 3; C, 4; D, 3; E, 3; F, 3.

Figure 7. CTF phosphorylation/dephosphorylation and its role in the NTF-CTF interaction. LPHN1 on the cell surface is cleaved and multiply phosphorylated. Both LPHN1 and RPTPσ are dimerized. Multimeric ligands (such as α-LTX, teneurin-2) can bring LPHN1 and RPTPσ into close proximity, which would facilitate CTF dephosphorylation and formation of SDS-resistant CTF complexes, but weaken the NTF-CTF interaction. Other protein phosphatases may also be involved.
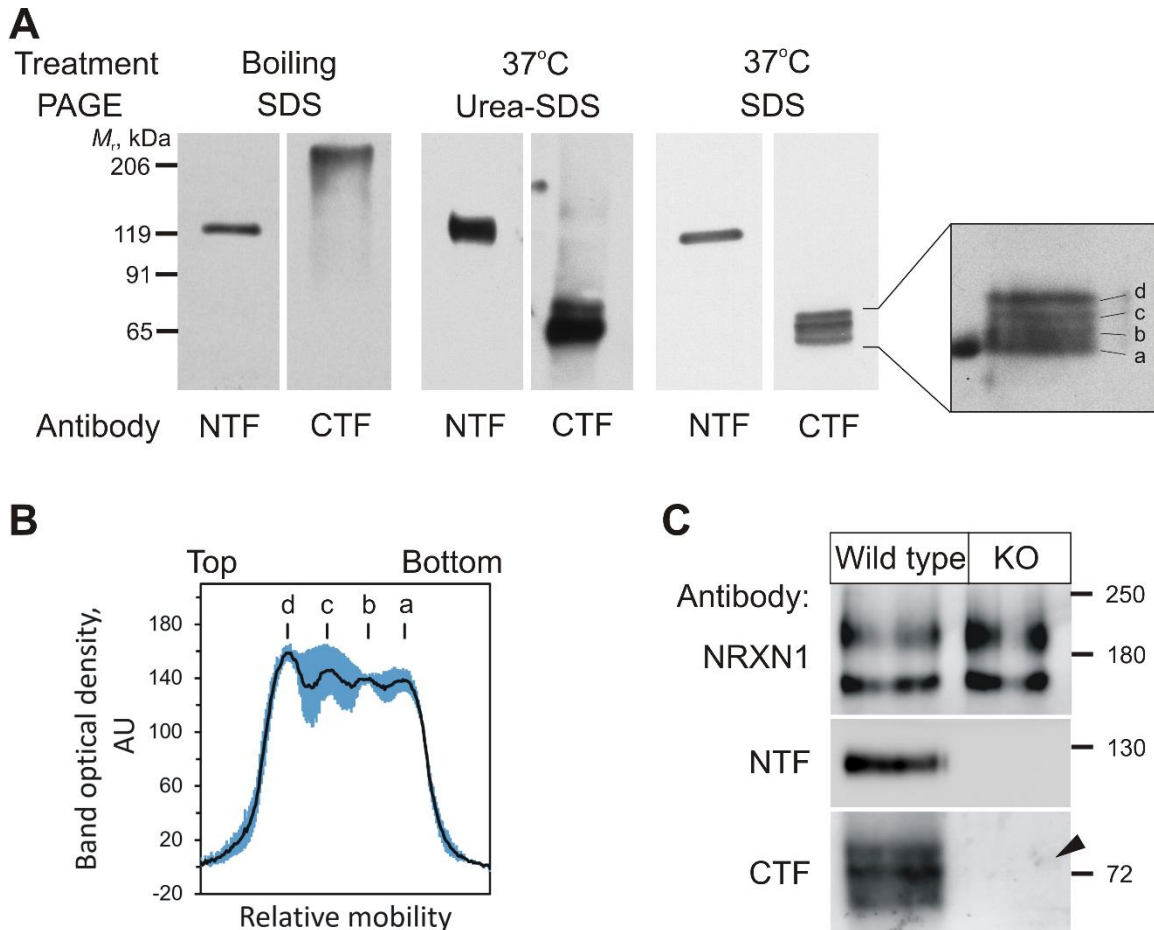
Figure 1. Analysis of the CTF of LPHN1 by SDS-PAGE. A. LPHN1 isolated on an α-LTX column from rat brain S1 membranes was separated in an 8% SDS-gel (conditions indicated at the top), and immunoblotted with antibodies against the NTF or CTF (shown at the bottom). Inset, electrophoretic separation of the CTF into 4 bands. **B.** Computer-aided densitometry of the CTF bands. Black line, an average profile; blue bars, standard deviation. **C.** Immunoblotting of brain membranes from wild-type and LPHN1 knockout (KO) mice for neurexin Iα (NRXN1), NTF and CTF. Arrowhead shows a lack of CTF staining in the KO brain. The numbers of independent experiments (*n*) were: A, 5; B, 6; C, 4.

Figure 2. The CTF of LPHN1 is phosphorylated on several sites. A. LPHN1 purified from S1 rat brain membranes on α-LTX was treated with neuraminidase and PNGase F or O-glycosidase, separated by SDS-PAGE and immunoblotted using affinity-purified antibodies against NTF and/or CTF. Inset, extended SDS-PAGE of LPHN1 in a 4% SDS-gel, immunoblotted for NTF. **B.** α-LTX-purified LPHN1 (left) or crude S1 membranes (right) were incubated with alkaline phosphatase (AP), in the absence or presence of exogenous PPIs. **C.** Computer-aided densitometry of the purified LPHN1 before (control) and after (AP) treatment with alkaline phosphatase. **D.** LPHN1 purified or from rat S1 membranes was treated with increasing doses of AP and hydroxylamine in the order shown. Right, a larger image of the blots showing lanes 2 and 3 to demonstrate that dephosphorylation of CTF induced its aggregation, but not degradation. Detergent extract from COS7 cells transiently transfected with LPHN1 was used as a marker of the dephosphorylated CTF. **E.** Quantification of all CTF-stained monomers and aggregates before (No AP) and after (AP) treatment with alkaline phosphatase. **F.** Purified LPHN1 treated (+) or untreated (−) with alkaline phosphatase was immunoblotted with antibodies against phosphorylated amino acids. **G.** Lanes 1, 2: synaptosomes (Syn) were incubated with ^{32}P orthophosphate, solubilized and used to isolate LPHN1, which was separated by SDS-PAGE, transferred onto PVDF membrane and autoradiographed for 40 h.

Lanes 3-5: the same blot as in lane 1 was immunostained for CTF and NTF; lane 4, long exposure. Lanes 6, 7: for comparison, purified LPHN1 was labeled with ^{125}I, blotted and autoradiographed for 16 h. Lanes 2, 7: the electrophoretic samples were boiled for 5 min before loading on SDS-gels. Filled arrowheads, CTF and CTF dimer (2); open arrowhead, NTF; asterisk, a phosphorylated contaminant; arrow, aggregated CTF at gel top (Aggr.). **H.** COS7 cells transiently expressing LPHN1 (or empty vector) were [^{32}P]-phosphorylated, separated by SDS-PAGE, transferred onto membrane and exposed to an X-ray film for 24 h (lanes 1, 2). The membrane was then immunostained for NTF and CTF (lanes 3-6). ^{32}P-labeled cellular proteins in control and LPHN1 cells are marked by asterisks. The immunoblot shows the uncleaved full-size LPHN1 (FS, black arrow), glycosylated (glyc.) and unglycosylated (unglyc.) NTF (open arrowheads) and the single CTF band (black arrowhead). Note that both the single CTF band and the FS LPHN1 are phosphorylated. The numbers of independent experiments (*n*) were: A, 4; B, 8/12; C, 8/12; D, 8; E, 8; F, 3; G, 3; H, 3.
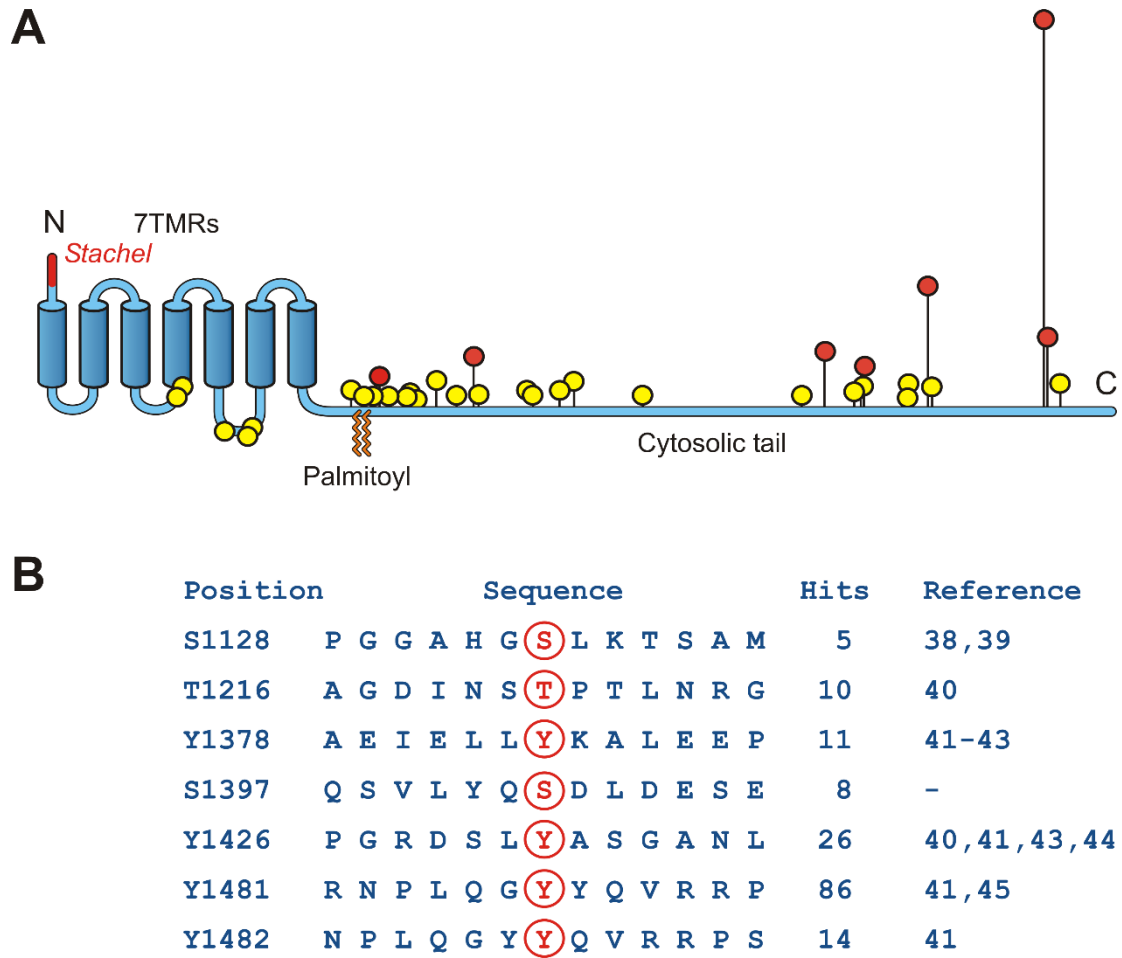
Figure 3. A map of predicted phosphorylation sites in the CTF. A. Phosphorylation sites predicted by high-throughput MS2[36] are indicated by circles, with the bar height proportional to the number of potential hits and the red color denoting sites with more than 5 hits. **B.** The positions and surrounding peptide sequences of the seven potentially phosphorylated residues (red circles in A); the predicted phosphorylated residues are encircled. The table also shows the number of theoretical hits and selected references reporting the predictions.

Figure 4. The CTF is dephosphorylated by cytosolic protein phosphatases and is lost from NTF. A. Brain membrane fractions (P1; S1; synaptosomes, Syn; and SPM) were solubilized in Thesit or CHAPS (for comparison of solubilization efficiency) and immunoblotted for NTF and CTF. LPHN1 expressed in COS7 cells was used as a marker of NTF and CTF proteins (labeling as in Fig. 2H). **B.** Differential abundance of the basally phosphorylated CTF-a (left) and maximally phosphorylated CTF-d (right) in respective brain membranes. t-Test with Bonferroni correction: *, p < 0.05. **C.** Inhibition of differential CTF dephosphorylation in the same membrane fractions by exogenous PPIs. **D.** CTF co-purifies with NTF on α-LTX columns from S1, but not from synaptosomes or SPM (two independent experiments with different exposure are shown). **E.** Quantification of CTF co-purifying with NTF on α-LTX-columns from respective membrane fractions. **F.** In the presence of exogenous PPIs, CTF co-purifies with NTF on α-LTX columns from all membranes. **G.** Alkaline phosphatase-induced dephosphorylation of CTF in S1 blocks its co-purification with NTF. H. The CTF in solubilized synaptosomes is not dephosphorylated and co-purifies with NTF on WGA-columns. **I.** Quantification of differential load affinity chromatography (example shown in Fig. 5A), in which the α-LTX column is either overloaded with an excess of LPHN1 in solubilized S1 membranes (>LPH) or is in excess over solubilized S1 (>LTX). t-Test with Bonferroni correction: ***, p < 0.001. **J.** Differential

52

load α-LTX-affinity chromatography with solubilized synaptosomes; the eluates are immunoblotted for NTF, CTF, and RPTPσ. The numbers of independent experiments (n) were: A, 3; B, 3; C, 6; D, 5; E, 5; F, 6; G, 3; H, 3; I, 5; J, 3.
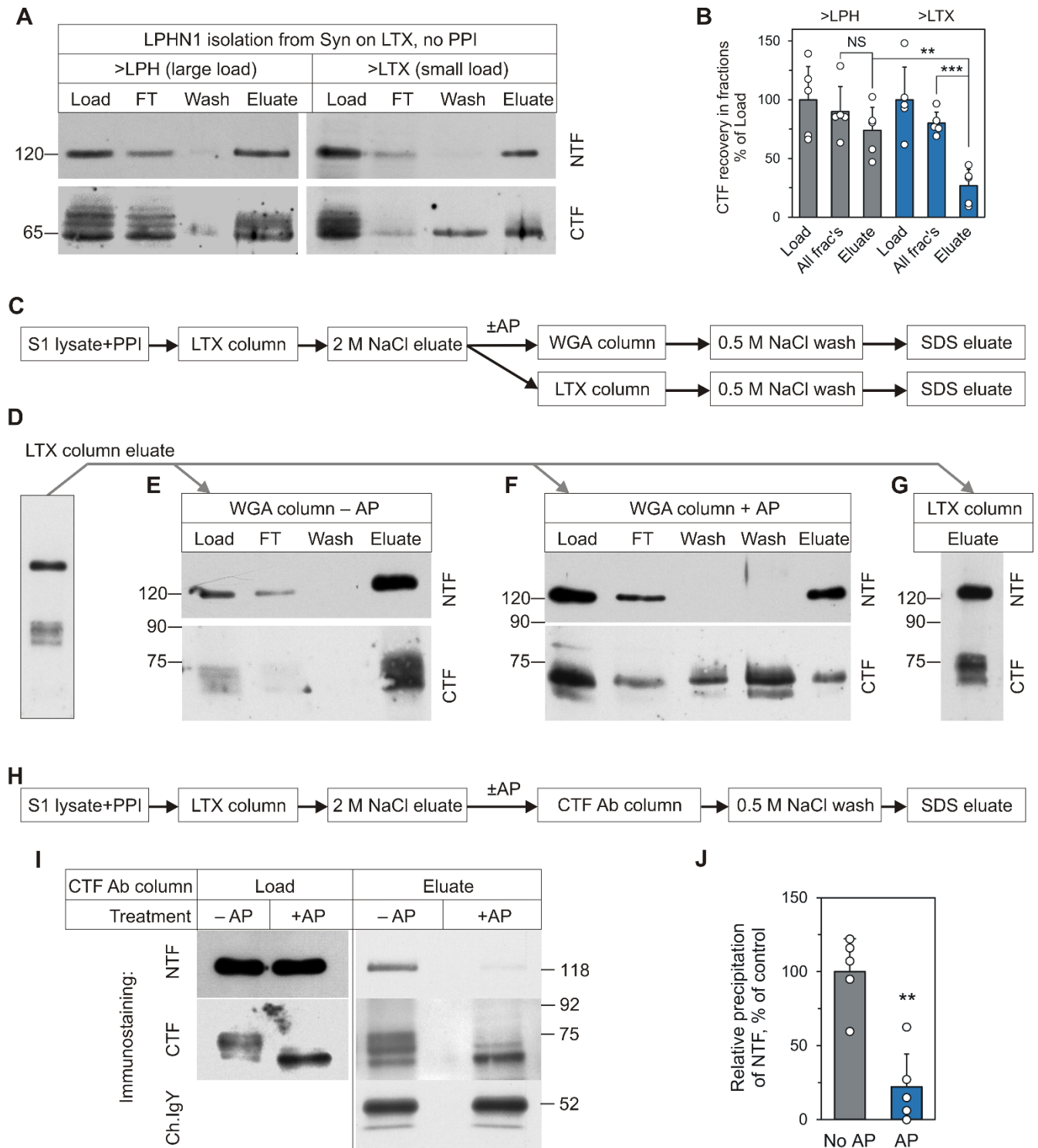
Figure 5. The CTF dephosphorylation decreases its high affinity for the NTF. A. Differential load α-LTX-affinity chromatography of solubilized synaptosomes. CTF is dephosphorylated during chromatography under >LTX condition and is released from the column in wash fractions. Overloading α-LTX-columns with LPHN1 in solubilized membranes blocks CTF dephosphorylation and dissociation from NTF. **B.** Quantification of differentia

load α-LTX-affinity chromatography experiments, as in A. t-Test with Bonferroni correction: **, $p < 0.01$; ***, $p < 0.001$. **C.** A scheme of experiments with secondary affinity chromatography of purified LPHN1 on α-LTX or WGA-columns, with or without alkaline phosphatase treatment. **D – G.** LPHN1 purified on α-LTX from S1 membranes was chromatographed on a WGA-column (with or without alkaline phosphatase, AP) or on an α-LTX column. **E, F.** WGA-chromatography of purified LPHN1 in the absence (**E**) or in the presence (**F**) of AP. **G.** Secondary chromatography of purified LPHN1 on an α-LTX column, in the absence of AP. Note that CTF is not dephosphorylated in the absence of other synaptosomal proteins. **H.** A scheme of immunoprecipitation experiments with LPHN1 purified from solubilized S1, with or without treatment with alkaline phosphatase, as shown in I. **I.** LPHN1 purified from S1 on an α-LTX-column was treated with or without alkaline phosphatase and immunoprecipitated using chicken anti-CTF antibodies and immunoblotted for CTF and NTF using respective rabbit antibodies. **J.** Quantification of experiments, as in I. The NTF yield in control experiments (No AP) taken as 100%. t-Test: **, $p < 0.01$. The numbers of independent experiments (*n*) were: A, 5; B, 5; D, 21; E, 3; F, 3; G, 3; I, 5; J, 5.
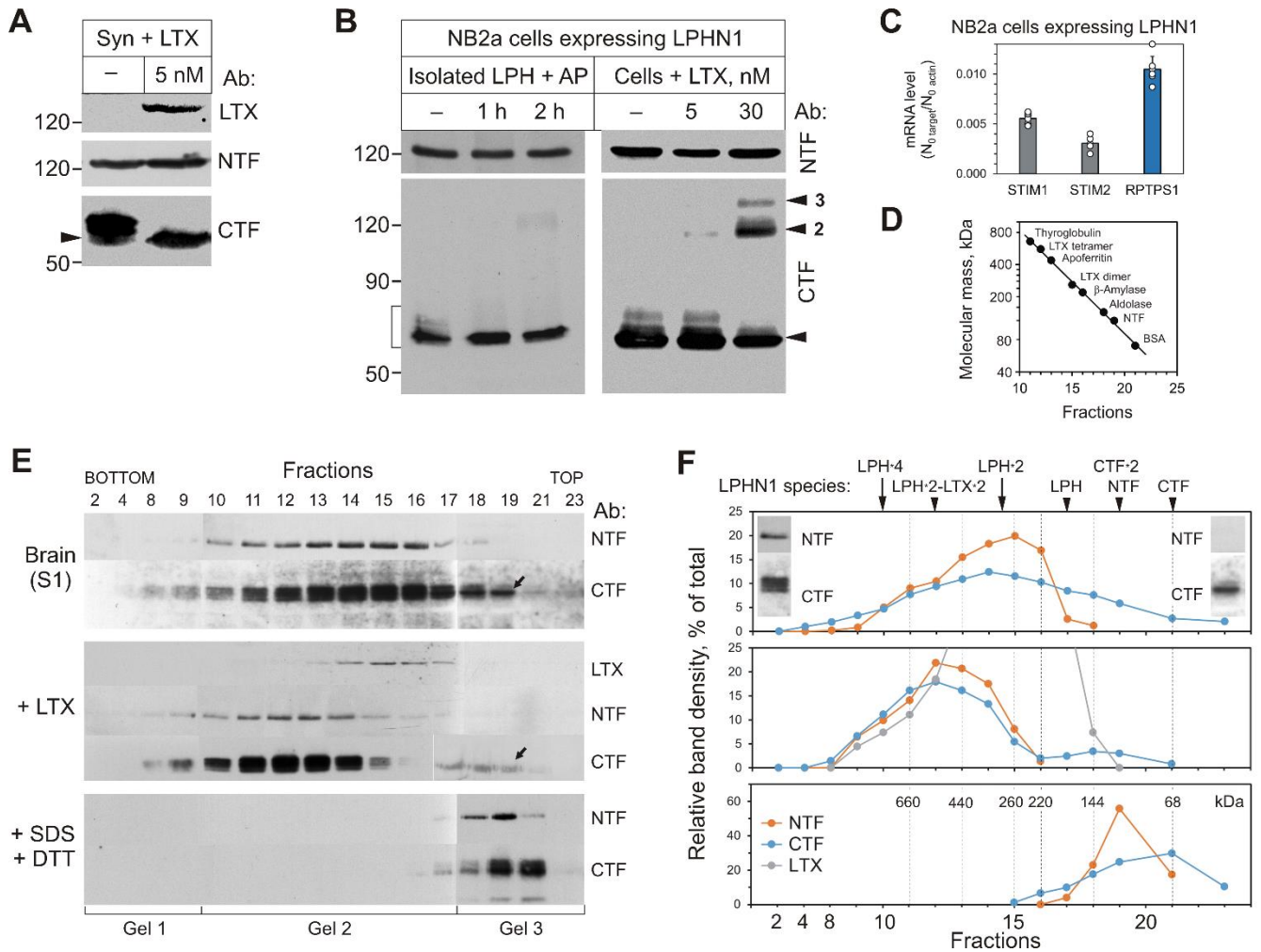
Figure 6. CTF dephosphorylation in cells and tissues. A. Synaptosomes were treated with 5 nM α-LTX for 1 h with oxygenation, then solubilized, separated by SDS-PAGE and immunoblotted for α-LTX, NTF and CTF. **B.** Left: LPHN1 purified from transfected NB2a cells was treated with alkaline phosphatase, separated by SDS-PAGE and immunoblotted for NTF and CTF. The CTF is phosphorylated, showing several differently migrating bands, which disappear on AP treatment. Right: LPHN1-expressing NB2a cells were incubated for 1 h with increasing amounts of α-LTX. α-LTX causes LPHN dephosphorylation and dimerization. **C.** RT-PCR analysis of RPTPσ mRNA in LPHN1-expressing NB2a cells. β-Actin mRNA was used for normalization, STIM1 and STIM2 used for comparison. **D.** Calibration curve for sucrose density gradients, as shown in E, using molecular mass marker proteins: thyroglobulin, apoferritin, β-amylase, α-LTX, aldolase, BSA. **E.** Rat brain membranes (S1) were solubilized in Thesit and centrifuged in sucrose density gradients, as described under Methods. The gradient fractions were separated by SDS-PAGE and immunoblotted for α-LTX (middle panel), NTF and CTF (3 gels were used to separate each gradient). Top, untreated solubilized S1 membranes. Middle, solubilized S1 membranes centrifuged in the presence of a large excess of α-LTX. Bottom, solubilized S1 membranes centrifuged after treatment with 1% SDS and 100 mM DTT. **F.** Quantification of NTF and CTF distribution in gradient fractions (from E). Insets,

56

LPHN1 at the bottom and top of gradient contains differentially phosphorylated CTF; only CTF is present in the top gradient fractions. The positions of predicted molecular species are shown at the top; the positions of molecular mass markers are shown in the bottom graph. The numbers of independent experiments (*n*) were: A, 4; B, 3; C, 4; D, 3; E, 3; F, 3.
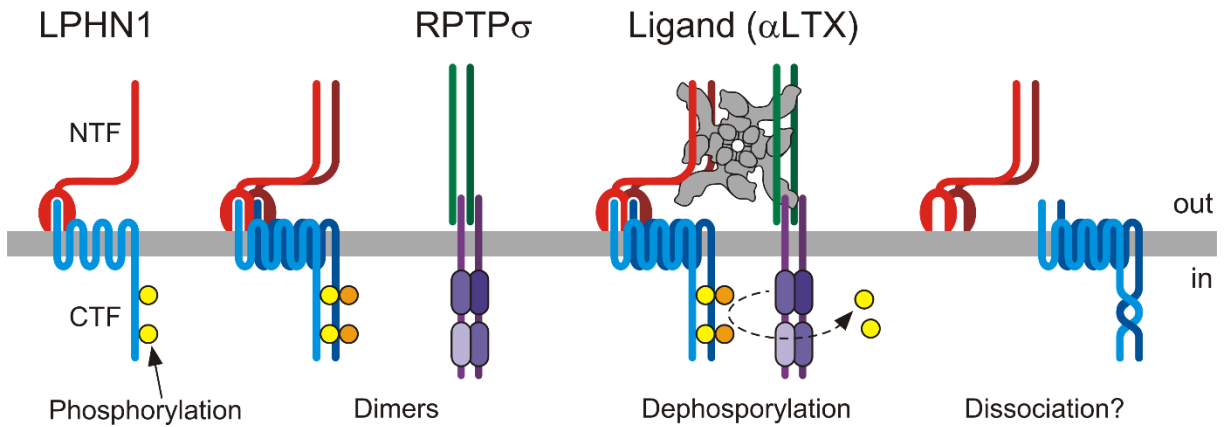
Figure 7. CTF phosphorylation/dephosphorylation and its role in the NTF-CTF interaction. LPHN1 on the cell surface is cleaved and multiply phosphorylated. Both LPHN1 and RPTPσ are dimerized. Multimeric ligands (such as α-LTX, teneurin-2) can bring LPHN1 and RPTPσ into close proximity, which would facilitate CTF dephosphorylation and formation of SDS-resistant CTF complexes, but weaken the NTF-CTF interaction. Other protein phosphatases may also be involved.